OXFORD

ORIGINAL ARTICLE

Biochemical, histological and functional correction of mucopolysaccharidosis Type IIIB by intra-cerebrospinal fluid gene therapy

Albert Ribera[1,2,†], Virginia Haurigot[1,2,†], Miguel Garcia[1,2], Sara Marcó[1,2], Sandra Motas[1,2], Pilar Villacampa[1,2], Luca Maggioni[1,2], Xavier León[1,2], Maria Molas[1,2], Víctor Sánchez[1,2], Sergio Muñoz[1,2], Christian Leborgne[5], Xavier Moll[3], Martí Pumarola[1,3], Federico Mingozzi[5,6], Jesús Ruberte[1,4], Sònia Añor[3] and Fatima Bosch[1,2,*]

[1]Center of Animal Biotechnology and Gene Therapy, [2]Department of Biochemistry and Molecular Biology, [3]Department of Animal Medicine and Surgery and [4]Department of Animal Health and Anatomy, School of Veterinary Medicine, Universitat Autònoma de Barcelona, 08193 Bellaterra, Spain, [5]Généthon, 91000 Evry, France and [6]University Pierre and Marie Curie, 75005 Paris, France

*To whom correspondence should be addressed. Tel: +34 935814182; Fax: +34 935814180; Email: fatima.bosch@uab.es

Abstract

Gene therapy is an attractive tool for the treatment of monogenic disorders, in particular for lysosomal storage diseases (LSD) caused by deficiencies in secretable lysosomal enzymes in which neither full restoration of normal enzymatic activity nor transduction of all affected cells are necessary. However, some LSD such as Mucopolysaccharidosis Type IIIB (MPSIIIB) are challenging because the disease's main target organ is the brain and enzymes do not efficiently cross the blood–brain barrier even if present at very high concentration in circulation. To overcome these limitations, we delivered AAV9 vectors encoding for α-N-acetylglucosaminidase (NAGLU) to the Cerebrospinal Fluid (CSF) of MPSIIIB mice with the disease already detectable at biochemical, histological and functional level. Restoration of enzymatic activity in Central Nervous System (CNS) resulted in normalization of glycosaminoglycan content and lysosomal physiology, resolved neuroinflammation and restored the pattern of gene expression in brain similar to that of healthy animals. Additionally, transduction of the liver due to passage of vectors to the circulation led to whole-body disease correction. Treated animals also showed reversal of behavioural deficits and extended lifespan. Importantly, when the levels of enzymatic activity were monitored in the CSF of dogs following administration of canine NAGLU-coding vectors to animals that were either naïve or had pre-existing immunity against AAV9, similar levels of activity were achieved, suggesting that CNS efficacy would not be compromised in patients seropositive for AAV9. Our studies provide a strong rationale for the clinical development of this novel therapeutic approach as the treatment for MPSIIIB.

Introduction

Mucopolysaccharidosis Type IIIB (MPSIIIB) or Sanfilippo syndrome Type B is an autosomal recessive Lysosomal Storage Disease (LSD) caused by insufficient activity of α-N-acetylglucosaminidase (NAGLU), one of the enzymes responsible for the lysosomal catabolism of the glycosaminoglycan (GAG) heparan sulphate (HS) [1]. In most cases (∼60%), the deficiency is caused by missense mutations affecting the catalytic site of the enzyme, resulting in the production of non-active proteins [2]. Small deletions/insertions, nonsense and splice site mutations have also been described in MPSIIIB patients [2,3]. The lack of adequate levels of enzymatic activity leads to the build-up of HS in lysosomes, and to secondary lysosomal dysfunction [4]. As a result of lysosomal pathology, cellular dysfunction and, eventually cell death occurs, affecting mostly the Central Nervous System (CNS) with additional peripheral tissue involvement [5,6].

After an asymptomatic period during the first few months of life, MPSIIIB patients generally manifest the disease with delayed intellectual development. The following phase is characterized by abnormal behaviour, sleep disturbances and neurocognitive decline associated with gradual speech loss [7]. By the time the disease advances to the development of dementia, behavioural alterations disappear, but motor functions progressively decline and eventually result in complete loss of locomotion and dysphagia among other symptoms [8,9]. The spectrum of somatic manifestations of MPSIIIB is broad and includes recurrent ear and respiratory tract infections, alterations of the digestive system with episodes of diarrhoea, skeletal abnormalities and mild hepatosplenomegaly [8,10]. Death generally occurs during the second or third decade of life [7,11], although less severe forms of the disease have a slower progression and longer life expectancy [9,12].

At present there are no drugs approved to treat MPSIIIB, and the clinical management of the disease is based on symptomatic and palliative treatments. Most therapeutic strategies under development are relying on cross-correction, based on the premise that NAGLU undergoes N-glycosylation of asparagine residues with mannose-6-phosphate (M6P) [13], which mediates uptake of the enzyme via M6P receptors located on the plasmatic membrane [14].

Enzyme replacement therapies (ERT) [15,16] and *in vivo* gene therapy approaches (ISRCTN19853672, www.controlled-trials.com) [17–19] have been proposed as treatments for MPSIIIB. ERT consists in the periodic administration of recombinant NAGLU [15]; however, as exogenously infused proteins do not easily cross the blood–brain barrier (BBB), the treatment of the CNS pathology with ERT would require the implantation of intrathecal devices to infuse the therapeutic protein directly in the cerebrospinal fluid (CSF).

Gene therapy can potentially overcome the limitations posed by the BBB and the short half-life of proteins by providing a continuous source of missing enzyme within the CNS. Promising results have been obtained using adeno-associated viral (AAV) vectors administered directly into the brain parenchyma, however, due to limited diffusion from the site of administration, to achieve widespread CNS transduction the vector has to be injected at multiple locations, complicating the surgical procedure [20,21]. In the context of MPSIIIB, direct intraparenchymal injection of AAV serotype 5 vectors has demonstrated efficacy in small and large animal models of the disease [17,22], and a clinical trial using this strategy has recently been initiated in MPSIIIB patients (ISRCTN19853672, www.controlled-trials.com). Aside from the highly invasive vector delivery method, this approach suffers

from obvious limitations associated with the impossibility to reach deeper areas of the encephalon and the lack of correction of peripheral disease.

Alternative gene therapy approaches to transduce the CNS take advantage of the properties of AAV9, a serotype with broad biodistribution capable of crossing the BBB when delivered to the bloodstream at high doses, resulting in the transduction of brain, as well as of liver, heart and, to a lesser extent, other organs [23,24]. This strategy has been tested in preclinical models of MPSIIIB leading to correction of the neurological and systemic pathology [18]. While these results are promising, large amounts of vector delivered systemically require considerable manufacturing efforts and may be associated with significant toxicities. Furthermore, transduction of brain via this route of administration is expected to be less efficient in large animals and humans compared with mice.

To address these important limitations, we and others have recently shown that it is possible to achieve widespread transduction of the CNS of small and large animals by administering AAV9 vectors directly into the CSF [25,26]. AAV9 outperformed all other serotypes tested, and distributed from the most rostral to the most caudal portions of the encephalon and down the spinal cord up to the cauda equina, leading to expression of the transgene in all key CNS structures [25]. Co-localization studies in dog brain samples using double-immunostainings with specific markers indicated that AAV9 transduced mostly neurons, with scarce transduction of astrocytes and no transduction of microglia [25]. Finally, AAV9 administration to the CSF also resulted in transduction of peripheral organs, mostly the liver, due to vector passage to the circulation [25,26]. This technique carries several advantages, including the use of a less invasive route of administration compared with intraparenchymal vector delivery and the need for lower vector doses compared with systemic vector administration. In the present work, we demonstrate the efficacy of intra-CSF delivery of AAV9-*Naglu* vectors in correcting neurological and somatic MPSIIIB disease, providing strong evidence of the therapeutic potential of this approach for the treatment of this disease and other LSDs that present with CNS and peripheral involvement.

Results

MPSIIIB mice have established disease at 2 months of age

We used a knock-out mouse model of MPSIIIB that closely recapitulates the pathological and clinical features of human disease [27–29]. This model completely lacks NAGLU activity (Supplementary Material, Fig. S1A–C), and has been extensively used to study the pathogenesis of MPSIIIB [27,28,30–35] and to test therapeutic approaches [18,22,29,36–42]. We chose to treat 2-month-old animals in order to mimic the clinical setting in which diagnoses arrives after GAG build-up has already caused appearance of symptoms. At 2 months of age, untreated MPSIIIB mice show considerable accumulation of GAGs in brain (40–110% over healthy WT levels, Supplementary Material, Fig. S1D), which leads to the enlargement of the lysosomal compartment (Supplementary Material, Fig. S1F) and causes a neuroinflammatory response with astrocytosis and microgliosis (Supplementary Material, Fig. S1G) similar to that described in human MPSIIIB [5,28,33]. GAG storage is also increased in peripheral tissues (Supplementary Material, Fig. S1E), in particular in liver, where GAG levels are 6-folds higher than in healthy animals and the size of the lysosomal compartment is markedly increased (Supplementary Material, Fig. S1H). Furthermore, MPSIIIB mice are more prone to suffer from anxiety
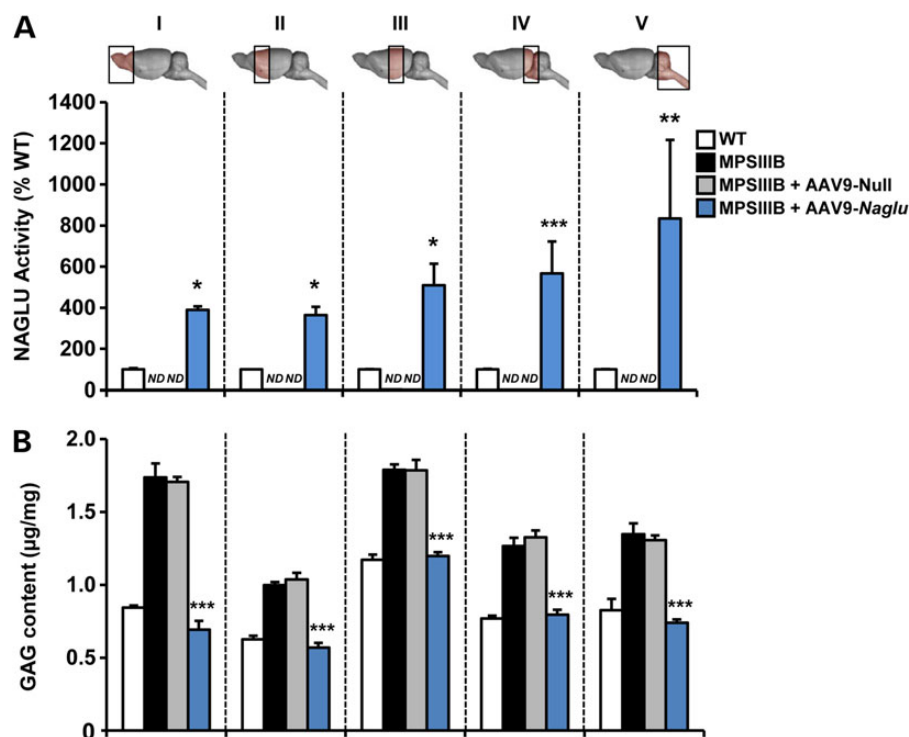
Figure 1. Restoration of NAGLU activity and correction of GAG storage following intra-CSF delivery of AAV9-*Naglu* vectors. Two-month-old MPSIIIB male mice were administered in the cisterna magna with 3×10^{10} vg of AAV9 vectors coding for codon-optimized murine NAGLU (AAV9-*Naglu*) or with non-coding vectors (AAV9-Null), as controls. Three months after treatment, brain samples from treated animals were harvested and analysed in parallel with samples from WT and untreated MPSIIIB littermates. (**A**) Percentage of WT NAGLU activity and (**B**) GAG content in the encephalon regions analysed (Sections I–V depicted in the diagrams above the plot). Results are shown as mean ± SEM of $n = 5$ animals/group. WT NAGLU activity was set to 100%, which corresponded to 0.93 ± 0.04, 0.79 ± 0.02, 1.00 ± 0.03, 0.97 ± 0.04 and 1.07 ± 0.04 nmol/h/mg protein for sections I–V, respectively. *$P < 0.05$, **$P < 0.01$ and ***$P < 0.001$ versus AAV9-Null. ND, non-detectable.

and are less exploratory in the Open-Field test, a well-established test used to evaluate locomotor activity and anxiety-related behaviour (43), evidencing behavioural deficits developed within 2 months from birth in this model (Supplementary Material, Fig. S2).

Intra-CSF delivery of AAV9-Naglu results in increased NAGLU activity and normalized GAG content in the CNS of MPSIIIB mice

We previously demonstrated that delivery of AAV9 vectors encoding sulphamidase to the CSF results in correction of MPSIIIA (25). To test the therapeutic potential of this approach in the context of MPSIIIB disease, we delivered 3×10^{10} vg/mouse of AAV9 vectors carrying a codon-optimized version of murine *Naglu*-coding sequence under the control of the chicken β-actin/CMV enhancer (CAG) ubiquitous promoter (AAV9-*Naglu*) to the cisterna magna of 2-month-old male and female MPSIIIB mice. Animals were sacrificed after 3 months of follow-up, i.e. at 5 months of age. In agreement with the comparable vector gene copy numbers documented throughout the CNS for both genders (Supplementary Material, Table S1), intra-CSF administration of AAV9-*Naglu* vectors resulted in high levels of NAGLU activity, ranging from 400 to 800% of values observed in healthy littermates, throughout the encephalon of MPSIIIB males (Fig. 1A) and females (Supplementary Material, Fig. S3A). Despite these high levels, no sign of overexpression-associated toxicity was observed in any part of the encephalon (Supplementary Material, Fig. S4). NAGLU activity remained undetectable, however, in untreated animals or in MPSIIIB mice that received noncoding AAV9 vector (AAV9-Null) used as control (Fig. 1A and Supplementary Material,

Fig. S3A). Co-localization studies in brain sections of mice injected intracisternally with AAV9 vectors encoding the reporter protein GFP and double-immunostained with specific markers for neurons (NeuN), astrocytes (GFAP) and microglia (Iba1) confirmed that AAV9 transduced mostly neurons in mice, with occasional transduction of astrocytes (Supplementary Material, Fig. S5).

Vector-derived NAGLU transgene expression led to complete normalization of GAG content in all CNS regions analysed, with AAV9-*Naglu*-treated MPSIIIB males and females showing similar levels of brain GAGs as wild-type controls (Fig. 1B and Supplementary Material, Fig. S3B), which represented a considerable reduction from GAG levels measured in untreated or Null-treated MPSIIIB mice (Fig. 1B and Supplementary Material, Fig. S3B).

Gene therapy restores normal size and function of CNS lysosomal compartment in MPSIIIB mice

Immunostaining of sections of the encephalon with an antibody directed against LIMP2, a protein integral to the lysosomal membrane commonly used as marker of these organelles (44,45), showed a remarkable decrease in signal intensity in treated MPSIIIB males and females in all CNS regions analysed, suggesting a reduction in the number and/or size of intracellular lysosomes (Fig. 2 and Supplementary Material, Fig. S6). These results were confirmed by ultrastructural analysis of the frontal cortex and cerebellum by transmission electron microscopy (TEM). Perineuronal glial cells of the cortex of untreated male and female MPSIIIB mice presented large electroluscent vacuoles that likely corresponded to lysosomes loaded with undegraded HS and other compounds (Fig. 3A and Supplementary Material,
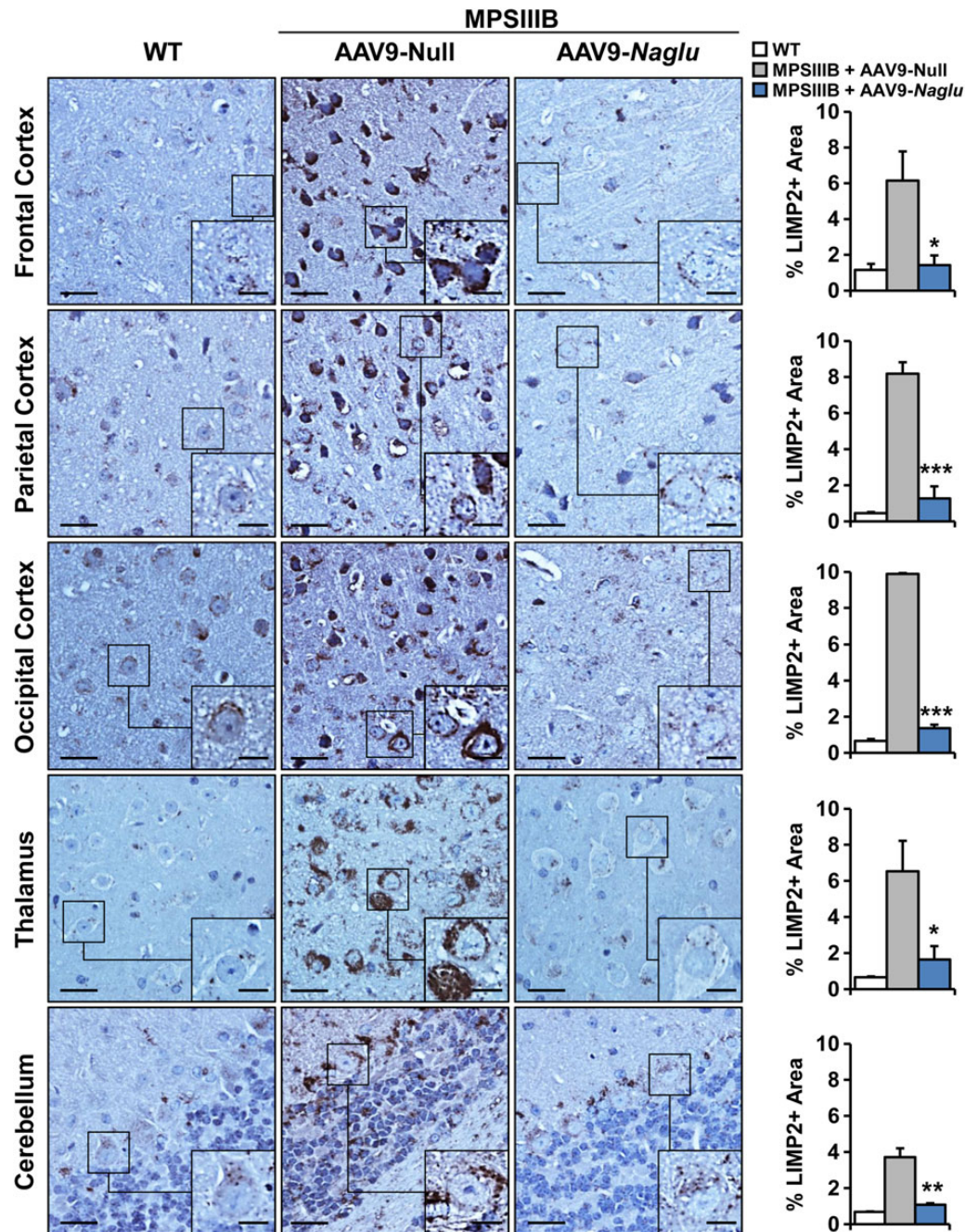
Figure 2. AAV9-*Naglu*-mediated reduction in the size of the CNS lysosomal compartment. Analysis of lysosomes in different regions of the brain and in cerebellum of WT, Null-treated or *Naglu*-treated MPSIIIB male mice by LIMP2 immunostaining. The compensatory expansion of the lysosomal compartment that characterizes the disease (AAV9-Null cohort, middle column) is completely counteracted by AAV9-mediated NAGLU gene transfer in all regions analysed. Scale bars, 25 μm and 10 μm (insets). Histograms on the right represent the quantification of the percentage of LIMP2+ area in each region for each treatment group. Data are shown as mean ± SEM, $n = 2$–3 animals/group. *$P < 0.05$, **$P < 0.01$ and ***$P < 0.001$ versus AAV9-Null.

Fig. S7A). In samples from AAV9-*Naglu* vector-treated male and female mice, perineuronal glial cells presented a wild-type appearance, with no discernible storage vesicles in their cytoplasm (Fig. 3A and Supplementary Material, Fig. S7A). In cerebellum, few but very large vacuoles were observed in somas of Purkinje neurons of untreated MPSIIIB animals, which were drastically reduced in size after AAV9-*Naglu* treatment (Fig. 3A and Supplementary Material, Fig. S7A), providing further evidence of effective clearance of GAGs by functional lysosomes.

In LSD, the activity of several lysosomal enzymes aside from that directly affected by the inherited mutation can be altered secondary to perturbation of normal lysosomal homeostasis (46). We observed that in the brain of untreated or Null-treated male and female MPSIIIB mice aged 5 months, the activities of *N*-sulphoglucosamine sulphohydrolase (SGSH), β-glucuronidase (GUSB) and β-hexosaminidase (HEXB) were significantly increased (Fig. 3B and Supplementary Material, Fig. S7B). Consistent with the reduction in GAG storage observed 3 months after
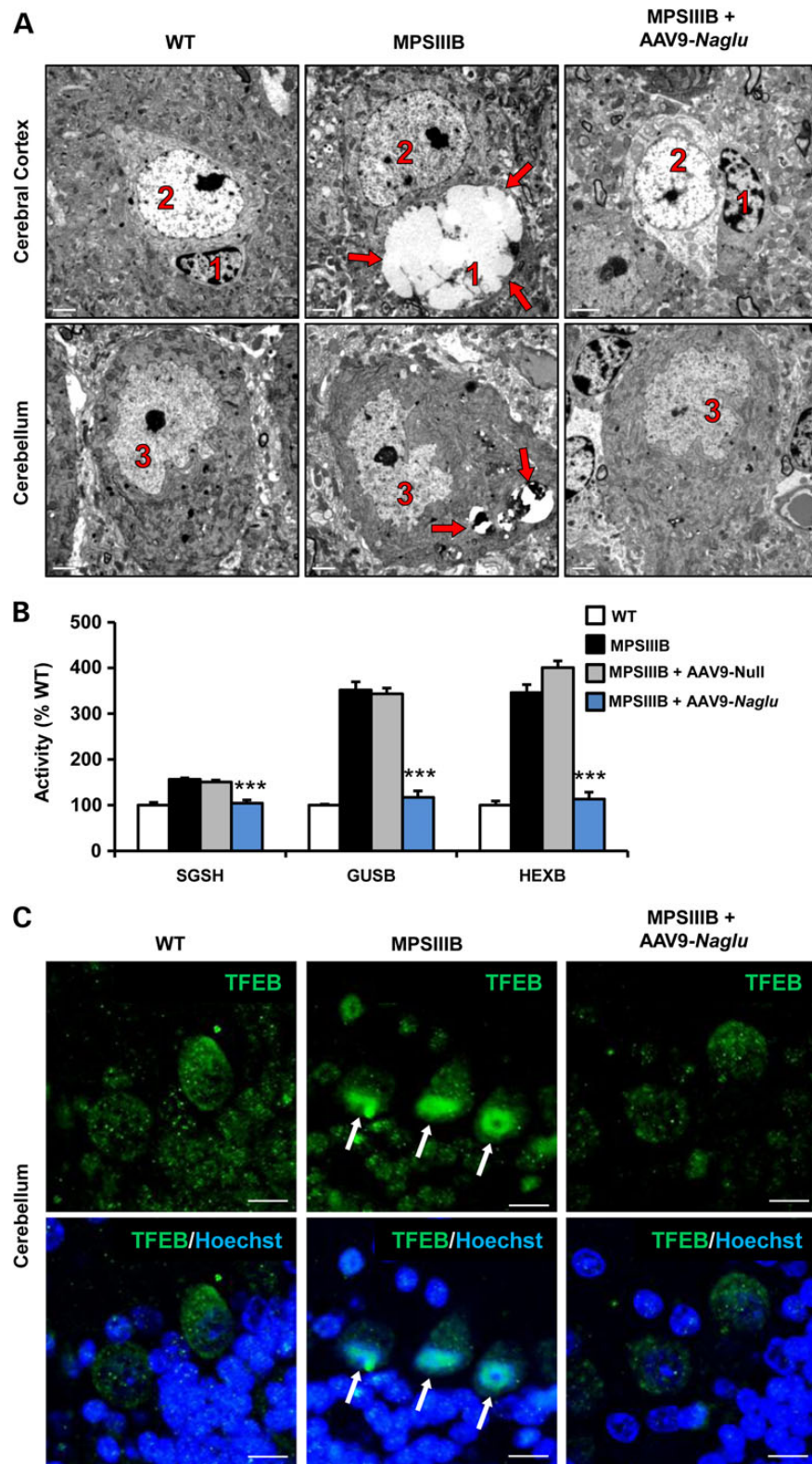
Figure 3. Restoration of CNS lysosomal homeostasis by AAV9-mediated *Naglu* gene transfer. (**A**) Ultrastructural analysis of cerebral cortex (top panels) and cerebellum (bottom panels) performed at 5 months of age in WT, untreated (MPSIIIB) and AAV9-*Naglu*-treated MPSIIIB (AAV9-*Naglu*) male mice showed an evident reduction in the size and number of intracytoplasmic electroluscent vacuoles (indicated by red arrows) in perineuronal glial cells (1) associated to neurons (2) of the occipital cortex and in Purkinje cells (3) of the cerebellum following AAV9-*Naglu* administration. Scale bars: 2 μm. (**B**) Activity, as % of WT, of other lysosomal enzymes different from NAGLU analysed 3 months after gene transfer. Intra-CSF delivery of AAV9-*Naglu* vectors restored the activities of SGSH, GUSB and HEXB in the brain of treated MPSIIIB males. Results are shown as mean ± SEM, *n* = 4 animals/group. ***P < 0.001 versus AAV9-Null. (**C**) Confocal analysis of TFEB immunostaining (green) in cerebellum sections of WT, untreated or *Naglu*-treated MPSIIIB male mice showing localization of TFEB to the nucleus (arrows) in untreated MPSIIIB animals but not in treated mice. Scale bars: 10 μm.

intra-CSF delivery of AAV9-*Naglu* vectors, the activity of brain SGSH, GUSB and HEXB returned to healthy wild-type levels in both genders (Fig. 3B and Supplementary Material, Fig. S7B).

Then we studied, by confocal analysis in cerebellum sections, the subcellular localization of Transcription Factor EB (TFEB), a master regulator of lysosomal biogenesis and function (46). In untreated MPSIIIB mice, TFEB clearly localized to the nucleus of Purkinje neurons (Fig. 3C) suggesting activation of an adaptive cellular response that attempts to compensate excessive GAG storage by boosting lysosomal function (47). In AAV9-*Naglu*-treated mice, TFEB was barely detectable in the nucleus (Fig. 3C). Altogether, these results indicated that NAGLU gene transfer was capable of completely reversing secondary lysosomal pathology in the brain.

Gene transfer with AAV9-Naglu corrects neuroinflammation in MPSIIIB mice

Neuroinflammation characterized by astrocytosis and microgliosis is a hallmark in MPSIIIB-affected animal models (28,33) and humans (5,6). Mouse brain sections were stained with an antibody specific for GFAP and with BSI-B4 lectin. GFAP is an astrocytic protein that is strongly upregulated upon activation of this cell type (48), and BSI-B4 has been reported to recognize α-D-galactose residues present on resting and activated microglia (49) but under our experimental condition preferentially labels amoeboid activated microglia (25,45,50). Both markers are commonly used to detect astrocytosis and microgliosis, respectively (26,44). At 5 months of age, AAV9-Null-treated MPSIIIB animals showed strong GFAP staining in different brain areas, with particularly intense signal in cortex, superior colliculus and thalamus (Fig. 4A and Supplementary Material, Fig. S8A). Treatment with AAV9-*Naglu* vectors mediated a statistically significant reversal of astrocytosis in all areas in both genders (Fig. 4A and Supplementary Material, Fig. S8A). On the other hand, BSI-B4 positive cells could be easily detected throughout the brain of 5-month-old Null-treated MPSIIIB animals (Fig. 4B and Supplementary Material, Fig. S8B). Microglial cells appeared to have large vacuoles in their cytoplasm in Null-treated MPSIIIB mice, a finding consistent with the observations made at ultrastructural level (Fig. 3A and Supplementary Material, Fig. S7A). Three months after delivery of AAV9-*Naglu* vectors, BSI-B4 signal almost disappeared from all brain areas of treated males (Fig. 4B) and females (Supplementary Material, Fig. S8B). Given that astrocytosis and microgliosis are already present at treatment (Supplementary Material, Fig. S1), results demonstrate that NAGLU gene transfer can reverse established neuroinflammation.

## AAV9-Naglu gene therapy normalizes the CNS gene expression profile

To further assess the efficacy of intra-CSF AAV9-*Naglu* gene therapy, we performed a gene expression profiling study using the Affimetrix® microarray platform on total RNA isolated from WT and AAV9-*Naglu* or AAV9-Null-treated MPSIIIB encephalon. After data processing and filtering, 94 genes were found to be differentially expressed among the three groups. The complete list of genes, as well as their fold-change with respect to the wild-type, is provided in Supplementary Material, Table S2. When Gene Ontology (GO) enrichment analysis was used to classify differentially expressed genes by biological process, 67 of the 94 genes were annotated with corresponding ontologies (Fig. 5B). Of these, the vast majority were associated with inflammation and innate immunity or functions that can be attributed to cells involved in these

processes. To confirm this observation, we used Cell Type Enrichment (CTEN) analysis to assess the contribution of different cell types to the observed changes in transcript levels. This software considers there is enrichment of a specific cell type if a software-defined score is greater than 2. The highest score for our data set was obtained for microglial cells (score = 60), a result in agreement with the important role attributed to microglia in neurodegenerative diseases and in MPSIII (28,51–54). When the effect of intra-CSF delivery of AAV9-*Naglu* vectors was evaluated, a striking change in the profile of gene expression with respect to AAV9-Null-injected animals was observed. Three months after vector administration, the vast majority of genes in treated MPSIIIB mice had transcript levels that resembled those of healthy littermates (Fig. 5A). Almost 90% of the genes differentially expressed in untreated MPSIIIB mice showed a correction in their transcript levels of at least 50% following AAV9-*Naglu* treatment and in 60% of them the correction was of 75%. Similar or slightly higher degrees of normalization in transcript levels were observed when the set of genes that the CTEN software had assigned to microglia was analysed separately (Fig. 5C). This observation supports the idea that microglia is largely responsible for the profile of gene expression observed in MPSIIIB and is in agreement with the complete reversal of microgliosis documented in treated animals (Fig. 4B and Supplementary Material, Fig. S8B).

## Delivery of NAGLU-coding vectors to the CSF of MPSIIIB mice results in correction of somatic pathology

Administration of AAV9 vectors to the CSF of mice and large animals results in liver transduction (25). Indeed, AAV9-*Naglu* vector genomes were detected in different lobes of the liver of injected mice (Supplementary Material, Table S1). Low but detectable copy numbers were documented in spleen and draining lymph nodes with minimal vector dissemination to other organs (Supplementary Material, Table S1). Importantly, no major differences were observed between AAV9-*Naglu*-injected wild-type and MPSIIIB mice (Supplementary Material, Table S1), suggesting that the underlying pathology does not affect peripheral vector distribution. As a consequence of vector spreading to the liver, hepatic NAGLU activity increased several folds in AAV9-*Naglu*-treated MPSIIIB mice; an average of 800% of wild-type levels was documented in males (Fig. 6A) and 250% in females (Supplementary Material, Fig. S9A) 3 months after vector delivery. Activity remained undetectable in livers of untreated and Null-treated MPSIIIB animals of both genders. The percent of transduced hepatocytes, quantified in mice injected with AAV9-GFP at a similar dose, was 3.97 ± 0.97%, similar to what was previously reported in dogs (25). There was no histological sign of NAGLU expression-associated toxicity in liver, and liver function tests were not altered by administration of NAGLU-encoding vectors (Supplementary Material, Fig. S10). Secretion of vector-derived NAGLU to the bloodstream resulted in increased activity in serum (Fig. 6B and Supplementary Material, Fig. S9B).

The restoration of peripheral enzyme activity led to complete normalization of pathological accumulation of GAGs in liver, spleen, heart and lung 3 months after gene transfer in both genders (Fig. 6C and Supplementary Material, Fig. S9C). A substantial reduction of GAGs was achieved in the urinary bladder (~70 and 55% for treated MPSIIIB males and females when compared with MPSIIIB Null-treated littermates), while a partial reduction of GAG content (~65% in males and ~20% in females) was observed in the kidney (Fig. 6C and Supplementary Material, Fig. S9C), an organ known to be refractory to cross-correction (18,25,26,50,55).
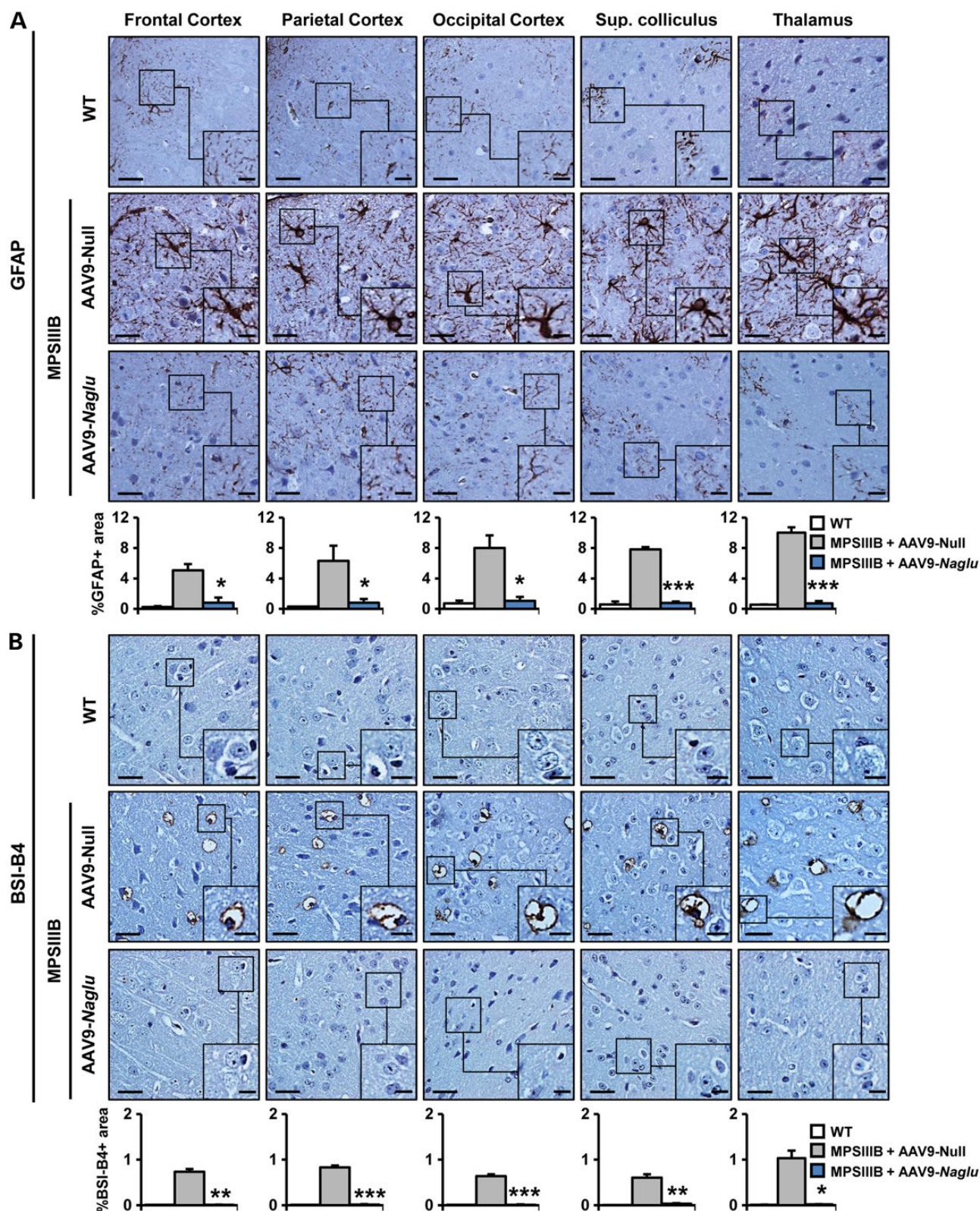
Figure 4. Disappearance of signs of neuroinflammation from the brain of MPSIIIB mice by intra-CSF treatment with AAV9-*Naglu* vectors. Evaluation of (**A**) astrocytosis by immunostaining for the astrocyte marker GFAP and (**B**) microgliosis by staining with lectin BSI-B4 of different brain regions from WT and Null (AAV9-Null) or AAV9-*Naglu*-treated MPSIIIB (AAV9-*Naglu*) males 3 months after gene delivery into the CSF. Images show a complete correction of neuroinflammation in all brain regions analysed in the treated group. Scale bars, 25 μm and 10 μm (insets). Histograms depict the quantification of positive signal area for each brain region in each cohort. Data are shown as mean ± SEM, $n = 2$–3 animals/group. *$P < 0.05$, **$P < 0.01$ and ***$P < 0.001$ versus AAV9-Null.
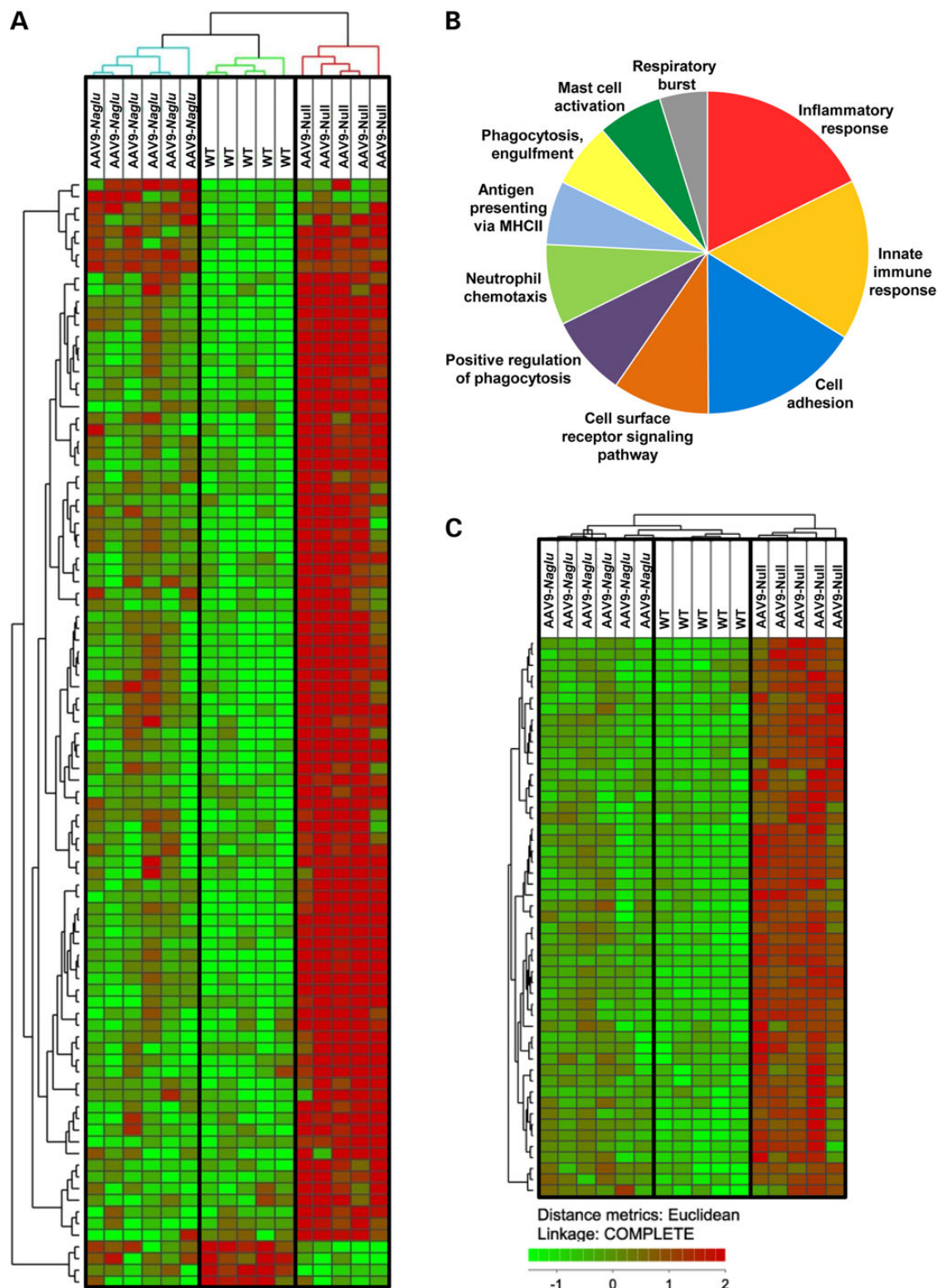
Figure 5. Normalization of CNS expression profile in treated MPSIIIB mice. Gene expression profiling of the CNS by microarray analysis performed 3 months after vector delivery to MPSIIIB male and female mice receiving either AAV9-Null or AAV9-*Naglu* vectors and in WT littermates. (**A**) Hierarchical clustering of all experimental groups based on the complete list of differentially expressed genes. Each row represents a gene and each column represents an animal. The level of expression of each gene is depicted relative to the mean abundance for that gene across all samples in a colour scale shown at the bottom. Red and green indicate transcript levels above and below the mean, respectively, and the magnitude of deviation from the mean is represented by the degree of colour saturation. The dendrogram of samples shown above the matrix represents overall similarities in transcript levels. Clearly, all AAV9-*Naglu*-treated MPSIIIB mice have a gene expression profile close to that of healthy, age-matched WT littermates. (**B**) Functional categorization based on GO annotation. Pie chart indicating the fraction of transcripts associated with each biological process term. Clearly, most of the terms represent inflammation/immunity-related categories. (**C**) Similar analysis by hierarchical clustering as in (A) of the set of genes that the CTEN software assigned to be representative of microglia.
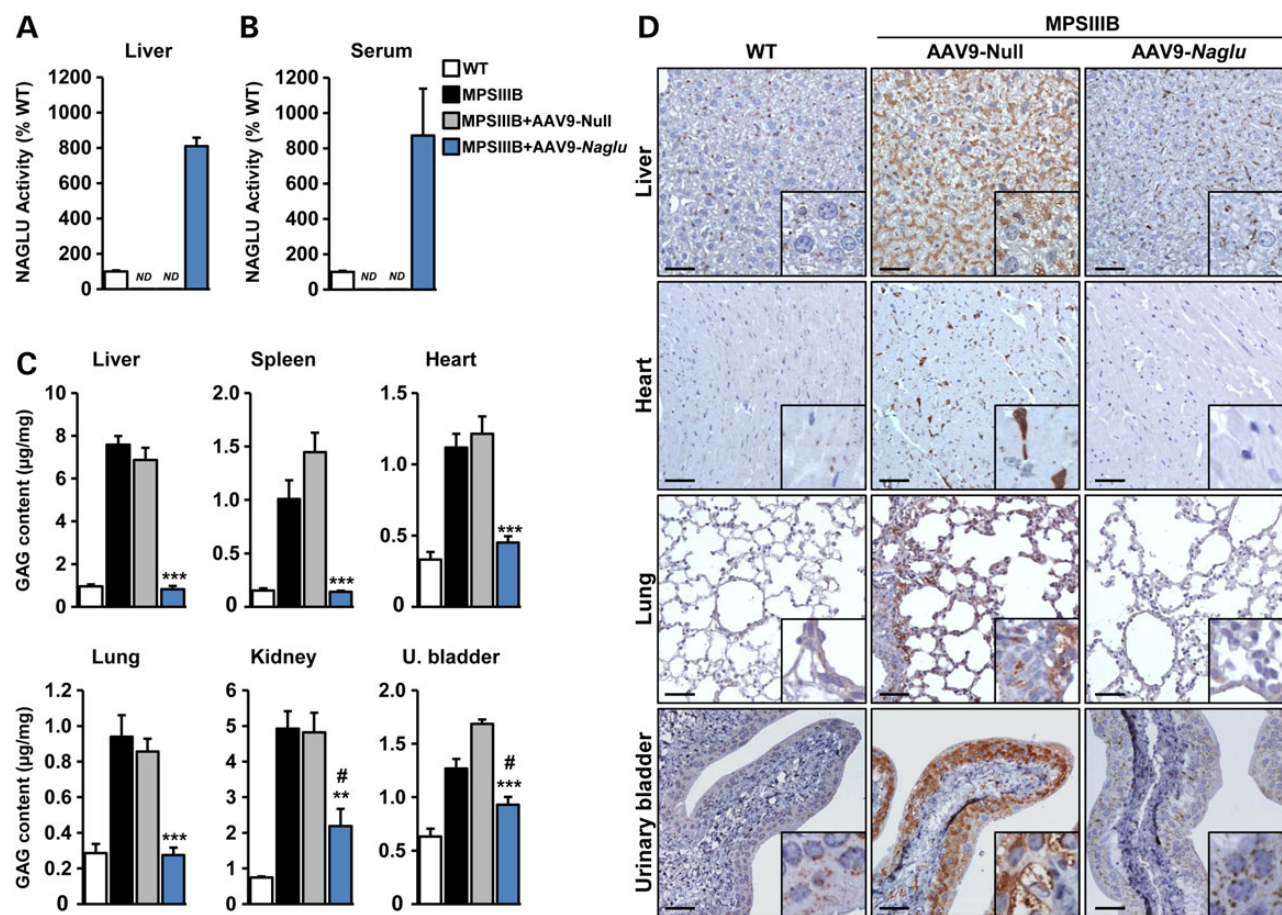
Figure 6. Effect of intra-CSF delivery of AAV9-*Naglu* on somatic pathology. (**A**) Liver and (**B**) serum NAGLU activity measured at 5 months of age in WT, untreated MPSIIIB or MPSIIIB males administered in the cisterna magna with AAV9-Null or AAV9-*Naglu* vectors. The levels of activity achieved in liver and serum were very similar suggesting that the liver is the main source of circulating enzyme. Activity is expressed as % of WT activity, which was set to 100%. (**C**) Quantification of GAG content in somatic organs in all experimental groups. Results are depicted as mean ± SEM. *n* = 5 animals/group. *$P < 0.05$, **$P < 0.01$ and ***$P < 0.001$ versus AAV9-Null; #$P < 0.05$ versus WT. ND, non-detectable. (**D**) Immunostaining against the lysosomal-associated protein LAMP1 in liver, heart, lung and urinary bladder from WT, Null-treated (AAV9-Null) or *Naglu*-treated MPSIIIB (AAV9-*Naglu*) male mice 3 months after vector delivery. Scale bars, 50 μm.

Consistent with the marked improvement in GAG accumulation, staining of tissue sections with anti-Lysosomal-Associated Membrane Protein 1 (LAMP1) antibody showed a clear reduction in the size of the lysosomal compartment in all somatic organs analysed in males (Fig. 6D) and females (data not shown). The study of liver ultrastructure by TEM confirmed the disappearance of storage vacuoles from the cytoplasm of treated MPSIIIB cells (Fig. 7A and Supplementary Material, Fig. S9D, right panels). Conversely, hepatocytes of MPSIIIB animals administered with non-therapeutic vector remained loaded with a large number of small electroluscent vacuoles (Fig. 7A and Supplementary Material, Fig. S9D, middle panels).

As observed in CNS, the clearance of storage material from the lysosomal compartment led to restoration of the activity of other lysosomal enzymes. In liver of untreated or Null-treated male and female MPSIIIB mice, the activities of α-iduronidase (IDUA), iduronate 2-sulphatase (IDS), SGSH, GUSB and HEXB were altered (Fig. 7B and Supplementary Material, Fig. S9E). Three months following AAV9-mediated NAGLU gene transfer, the activity of all these enzymes returned to normal levels in both genders (Fig. 7B and Supplementary Material, Fig. S9E), further supporting the concept that CSF gene transfer of NAGLU can reverse disease phenotype also in peripheral organs.

Intra-CSF AAV9-Naglu therapy restores normal behaviour and survival of MPSIIIB animals

At treatment, MPSIIIB mice already show behavioural deficits in the Open-Field test (Supplementary Material, Fig. S2). At 5 months of age, MPSIIIB animals naïve to the test either untreated or Null-vector injected took longer to enter the centre of the arena for the first time and subsequently did so less frequently than wild-types, spending more time at the border of the field and avoiding the central zone of the arena, which is the most anxiogenic zone (Fig. 8A). Untreated MPSIIIB animals also spent more time resting, travelled less distance and crossed fewer lines of the arena than wild-type aged-matched littermates, evidencing reduced exploratory and locomotor activity (Fig. 8A and Supplementary Material, Fig. S11A). The administration of NAGLU-encoding AAV9 vectors to the CSF of MPSIIIB mice led to the restoration of normal behaviour in both genders (Fig. 8A and Supplementary Material, Fig. S11A). No statistical differences were observed in any of the parameters measured between wild-type and NAGLU vector-treated MPSIIIB mice. Altogether, these observations indicate that under the experimental conditions of this study the intra-CSF delivery of AAV9-*Naglu* vectors is capable of reversing the cognitive changes induced by MPSIIIB disease.
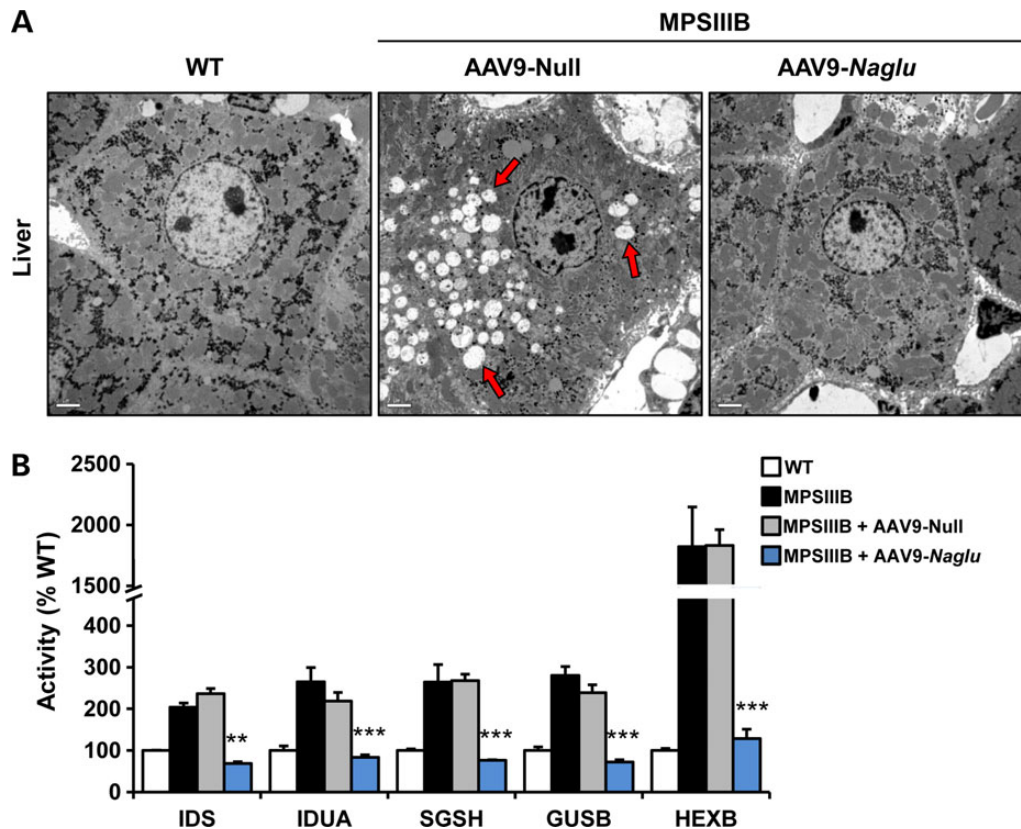
Figure 7. Normal structure and function of hepatic lysosomes in AAV9-*Naglu*-treated animals. (**A**) Transmission electron microscopy of the liver demonstrating the correction of the distension of the hepatic lysosomal compartment (arrows) in MPSIIIB male mice that received a single intra-CSF administration of AAV9-*Naglu* vectors at 2 months of age (right panel). Scale bars, 2 μm. (**B**) Intra-CSF AAV9-*Naglu*-mediated restoration of the normal level of activity of other lysosomal enzymes whose function in the liver is altered secondary to NAGLU deficiency. Activities are represented as % of WT (set to 100%). Results are shown as mean ± SEM. $n = 4$ animals/group. **$P < 0.01$ and ***$P < 0.001$ versus AAV9-Null.

Finally, we assessed the impact of intra-CSF AAV9-*Naglu* vector administration on animal survival as a measure of functional correction. Untreated or Null-treated MPSIIIB males showed a median survival of 14 and 13.9 months, respectively, all animals being dead by 17 months (Fig. 8B). Untreated or Null-treated MPSIIIB females lived slightly less, with a median survival of 11.7 months for untreated and 11.2 months for Null-injected MPSIIIB (Supplementary Material, Fig. S11B). All MPSIIIB females that did not receive therapeutic vector were dead by the age of 15 months. MPSIIIB animals receiving AAV9-*Naglu* vectors lived significantly longer than untreated MPSIIIB mice. Treated males showed a median survival of 21 months ($P = 0.0004$ versus Null-injected males), with some animals living up to 29 months (Fig. 8B). Similarly, treated MPSIIIB females had a median survival of 20.9 months ($P < 0.0001$) (Supplementary Material, Fig. S11B). Median survival for healthy male and female littermates was 26.7 and 24.9 months, respectively. The longer lifespan of treated MPSIIIB mice further demonstrates the therapeutic potential of intra-CSF AAV9-*Naglu* delivery.

Effect of pre-existing immunity on the levels of NAGLU activity in the CSF

The presence of neutralizing antibodies (NAbs) in the serum of a large proportion of the human population (56) is a serious limitation to AAV-mediated gene transfer after systemic administration (57–59). However, immunoglobulins are found at lower concentration in the CSF than in circulation due to the existence of the BBB that prevents most plasma proteins from entering the CNS. Although it has been suggested that the BBB is disrupted in patients affected by LSD (60), we have shown that the asymmetrical distribution of anti-AAV NAbs across the BBB of patients suffering from Sanfilippo Syndrome is preserved even in severely affected children (25). To provide a sensitive readout of the effect of anti-AAV NAbs in the setting of AAV9 gene transfer for MPSIIIB, two adult healthy Beagle dogs (Dogs 1 and 2) were immunized by intravascular injection of 1.2×10^{12} vg of AAV9-Null vector. Six weeks after vector delivery Dogs 1 and 2 had NAb titres in serum that ranged from 1:100 to 1:1000 (Fig. 9A). In contrast, naïve animals (Dogs 3 and 4) had undetectable levels of circulating NAbs (Fig. 9A). At this time, paired CSF samples were negative for NAbs in all animals (Fig. 9A). We then administered 6.5×10^{12} vg of AAV9 vectors encoding for canine NAGLU (AAV9-c*Naglu*) to the cisterna magna of the four dogs. Upon vector delivery, NAb titres quickly rose in serum of naïve animals (Dogs 3 and 4) to levels similar to those found in pre-immunized dogs (Dogs 1 and 2); in CSF NAbs remained undetectable in all dogs (Fig. 9A). Periodic sampling of CSF was performed to monitor transgene expression up to 18 weeks. A considerable increase above NAGLU basal activity levels was documented in all dogs, regardless of the presence of circulating NAbs in serum at the time of administration (Fig. 9B). NAGLU activity reached peak levels approximately 14 days post vector delivery and gradually decreased during the ensuing weeks, reaching stable levels by week 13 (Fig. 9B). Importantly, the administration of AAV9-c*Naglu* vectors was well tolerated in both naïve and pre-immunized dogs, and CSF
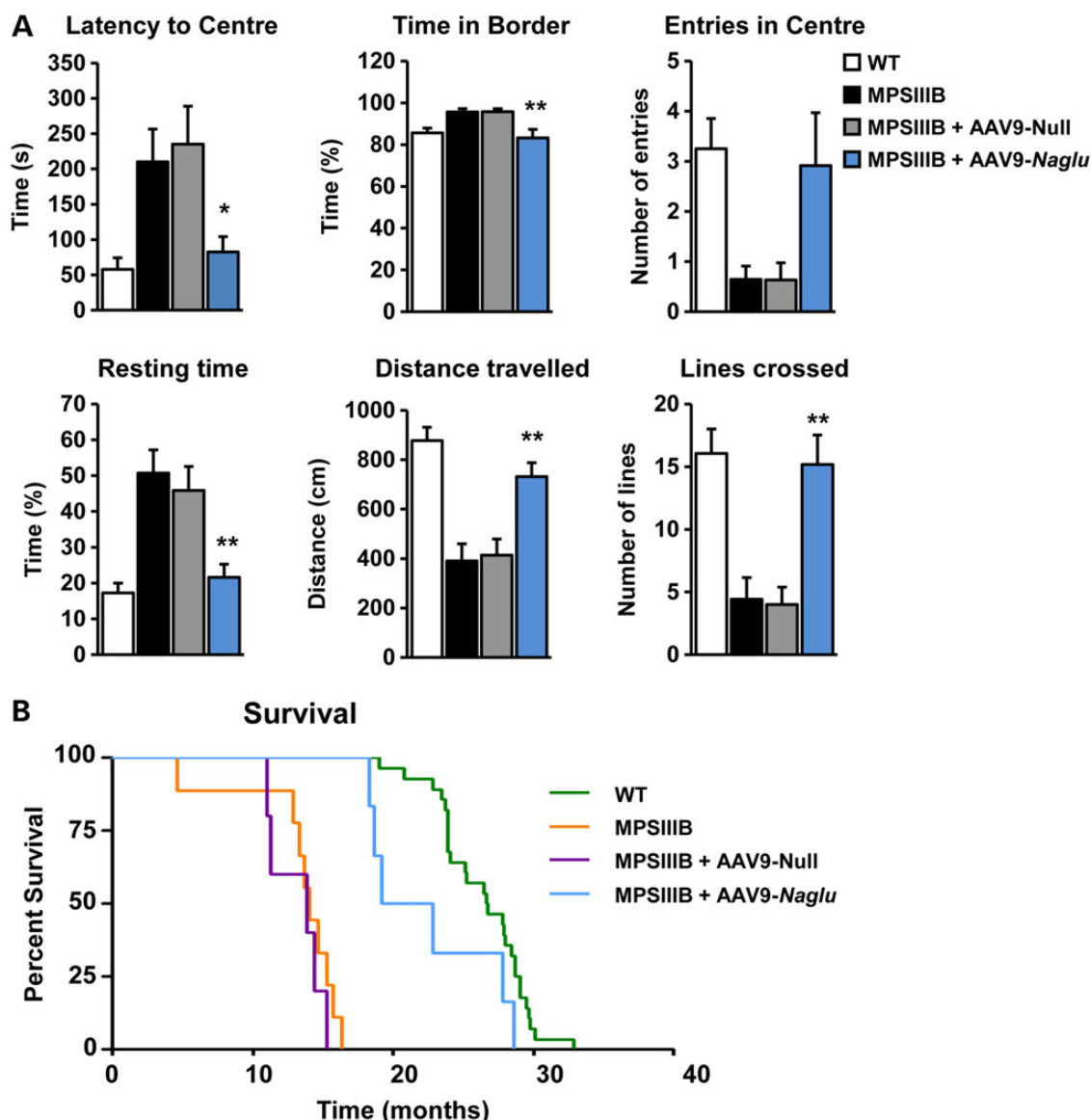
Figure 8. Behavioural correction and prolonged survival following AAV9-*Naglu* intra-CSF administration. (**A**) Results of the Open-field test performed in naïve-tested WT, untreated, and AAV9 vector (Null or *Naglu*) treated MPSIIIB male mice at 5 months of age. Histograms represent the mean ± SEM obtained during the first 2 min of recording for each parameter in groups of 12–15 animals/cohort. *$P < 0.05$ and **$P < 0.01$ versus MPSIIIB–Null. Intracisternal delivery of AAV9-*Naglu* vectors corrected anxiety-related behaviour (latency to centre, time in border and entries in centre) and normalized exploratory activity (resting time, distance travelled and lines crossed) in MPSIIIB males whose behaviour was indistinguishable from that observed in WT littermates. (**B**) Kaplan–Meier survival analysis in all experimental groups. Median survival was 26.6, 14, 13.9 and 21 months for, WT ($n = 28$), MPSIIIB ($n = 9$), AAV9-Null ($n = 5$) and AAV9-*Naglu* ($n = 8$), respectively. $P = 0.0004$ for AAV9-Null versus AAV9-*Naglu* treated MPSIIIB mice; $P = 0.0275$ for AAV9-*Naglu* versus WT.

white blood cell counts and total protein levels remained within normal range (Supplementary Material, Table S3) in all animals, indicating absence of vector-induced CNS inflammation. Likewise, the periodic monitoring of haematological, biochemical and liver functional parameters always showed values within the normal range in all dogs (data not shown). Together these results demonstrate that intra-CSF delivery of AAV9 vectors is safe and efficient even in the presence of high-titre serum NAbs (>1:1000).

Discussion

Intra-CSF delivery of AAV9-Naglu vectors to treat MPSIIIB

MPSIIIB represents a high unmet medical need, as no specific treatment has yet been approved that can modify the natural

history of this devastating condition. Gene therapy is an attractive tool for the treatment of LSD caused by deficiencies in secretable lysosomal enzymes in which neither full restoration of normal enzymatic activity nor transduction of all cells of the affected organ are necessary. However, some LSD such as MPSIIIB represent a difficult challenge because the disease's main target organ is the brain and enzymes do not efficiently cross the blood–brain barrier even if present at very high concentration in circulation. We here report on a novel approach to treat MPSIIIB based on the intra-CSF delivery of AAV9 vectors encoding for NAGLU. Long-term efficacy was documented in a mouse model that recapitulates the human disease at biochemical, histological and functional level and the approach was demonstrated to be scalable and safe in a large animal model. The success of this strategy is partly based on the properties of AAV9, a vector serotype with
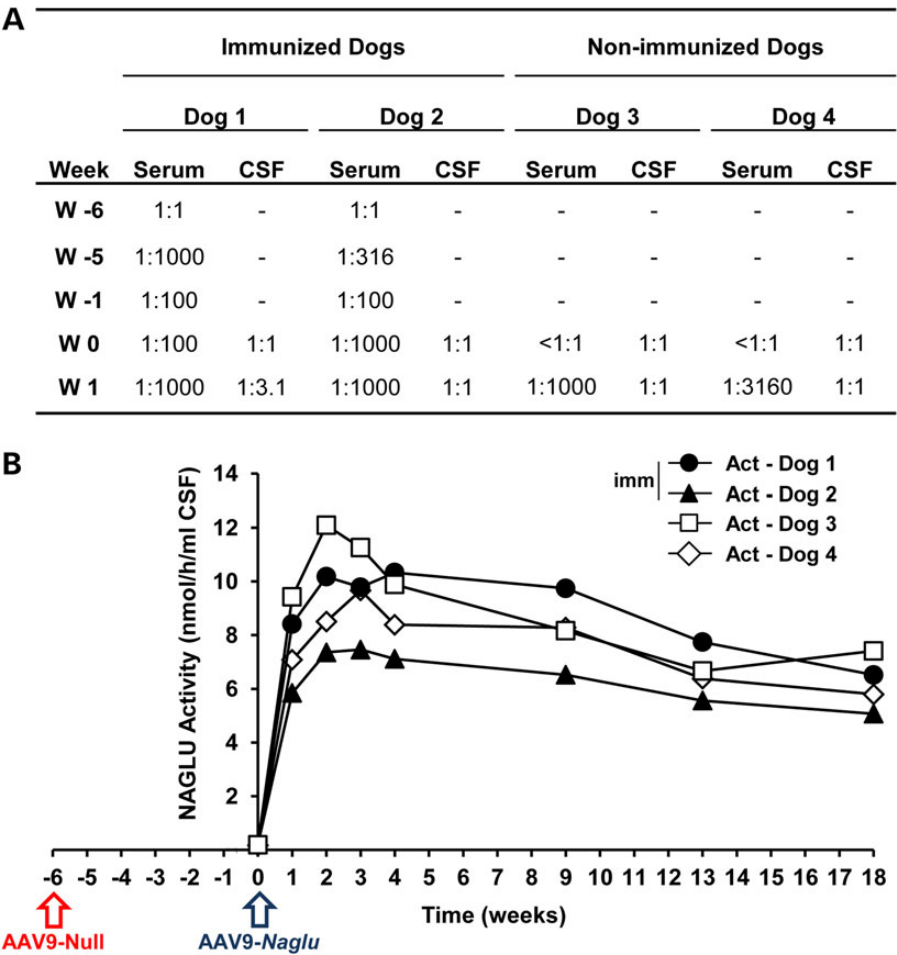
Figure 9. CSF levels of NAGLU activity in dogs are not affected by pre-existing anti-AAV9 humoral immunity. (**A**) Follow-up of NAb titres in matched CSF and serum samples before and after intra-CSF delivery of AAV9-*Naglu* vectors to naïve and pre-immunized dogs. For immunized dogs, the '0' time point corresponds to samples obtained before intra-CSF administration, i.e. 40 days after immunization by intravenous delivery of 1.0×10^{11} vg of AAV9-Null vector. (**B**) Monitoring of enzymatic activity in the CSF after intracisternal delivery of 6.5×10^{12} vg of AAV9 vectors encoding for canine NAGLU to healthy adult dogs that had pre-existing anti-AAV9 immunity (Dogs 1 and 2, filled symbols) or that were naïve to the vector (Dogs 3 and 4, open symbols) at the time of intra-CSF vector delivery. Basal CSF NAGLU activity was quantified in all dogs before vector administration and was in average below 0.22 nmol/h/ml CSF.

broad tropism (24,61). This, combined with intra-CSF delivery, maximized distribution of the vectors in the main target organ of the disease, the brain, but also transduced somatic organs, allowing for a considerable dose reduction (>8-fold reduction) over systemic delivery to achieve neurological and somatic correction of MPSIIIB (18). In addition, this route of delivery achieves widespread CNS and PNS transduction (25) with a surgical procedure that is standard practice in paediatric neurosurgery (62), in clear advantage over approaches in which the vector is delivered to the CNS parenchyma at multiple sites (20).

Efficacy and safety of intra-CSF delivery of AAV9-Naglu vectors

At the doses of AAV9-*Naglu* vectors used in this study, we achieved very high levels of NAGLU activity in the encephalon of male and female MPSIIIB mice, which mediated complete clearance of excessive GAGs in the CNS. The use of a codon-optimized transgene in combination with the intra-CSF route of delivery allowed levels of NAGLU activity in the brain far superior to those achieved by intravenous administration of the same serotype (18). Very high levels of circulating enzymatic activity

were also documented after CNS-directed delivery of AAV9-*Naglu* vectors, although at lower levels in MPSIIIB females than in males. This observation can be attributed to androgen-driven differences in the efficiency of liver transduction by AAV vectors in rodents (25,45,50,63), which do not seem to occur in non-human primates (64). Despite the supraphysiological levels of enzyme achieved in the CNS and periphery, there was no sign of NAGLU-mediated toxicity in treated mice. Indeed, GAG levels were normalized in treated animals, indicating that vector-derived NAGLU only acted on HS that was being metabolized in the lysosome. The fact that lysosomal enzymes are active only at the low pH (<5) of the lysosome constitutes an advantageous safety feature in the development of therapeutic approaches for LSD, as in certain cases high levels of circulating enzyme may be desirable to reach hard-to-treat organs, such as kidney, heart valves or bone (26,65–68). Furthermore, when the dose of vector used in the proof-of concept studies in MPSIIIB mice was extrapolated by brain volume to dogs, NAGLU activity measured in the CSF persisted at levels 25–40 folds higher than pre-treatment over the 18-week follow-up period, but all animals remained clinically well and there was no sign of CNS inflammation or peripheral toxicity. Nevertheless, given that preclinical studies in other

forms of MPS have demonstrated that levels of circulating enzyme as low as 5% of normal can correct pathological GAG accumulation (66,67), further studies to fine-tune the therapeutic dose of AAV9-*Naglu* are warranted before the translation of our approach to the clinic.

Restoration of normal lysosomal homeostasis by intra-CSF AAV9-Naglu treatment

As scientific understanding of LSDs improved in recent years, it has become evident that lysosomal dysfunction in LSDs goes beyond the simple accumulation of an undergraded substance whose catabolism is blocked due to an enzymatic deficiency. For example, mounting evidence from different animal models of LSD describes the secondary accumulation of unrelated compounds, such as GM2 and GM3 gangliosides or cholesterol in the case of MPSIIIB (27,33,69,70). Studies at cellular level demonstrate that this secondary storage is located in vesicles different from those that accumulate GAGs (71) suggesting this process is not the direct consequence of abnormal storage but rather the result of a general perturbation of cellular physiology due to lysosomal dysfunction. Lysosomes have now emerged as central organelles that participate in plasma membrane repair, intracellular trafficking, nutrient sensing, phagocytosis, autophagy and innate and adaptive immunity (47,54), and they are involved in the pathogenesis of other neurodegenerative diseases besides LSD, such as Alzheimer and Parkinson (72,73). The loss of lysosomal homeostasis due to disease elicits an adaptive cellular response that attempts to boost lysosomal function by increasing lysosomal biogenesis and hydrolases activities through binding of the transcription factor TFEB, a master regulator of lysosomal function, to the Coordinated Lysosomal Expression and Regulation (CLEAR) element present in the promoter of a number of genes encoding lysosomal proteins (46). Indeed, we observed translocation of TFEB to the nucleus of MPSIIIB brain cells demonstrating the activation of this response in MPSIIIB animals. The delivery of NAGLU-coding AAV9 vectors to the CSF of MPSIIIB mice had several effects on the lysosomal compartment. First, by restoring lysosomal NAGLU activity it cleared pathological GAG storage from CNS and somatic organs. Second, it reduced the expansion of the lysosomal compartment, as evidenced by staining with the specific lysosomal markers LIMP2 and LAMP1 in CNS and peripheral tissues, respectively, and by TEM in brain, cerebellum and liver. Finally, NAGLU gene transfer restored the normal levels of activity of several lysosomal enzymes in the brain and liver. The normalization of enzymatic activities that are not directly involved in HS degradation indicates that intra-CSF AAV9-*Naglu* therapy not only got rid of excessive HS storage but also restored normal lysosomal physiology. In agreement with this, in AAV9-*Naglu*-treated animals, TFEB localized to the cytoplasm and not the nucleus in brain cells.

Role of microglia in MPSIIIB and effect of intra-CSF AAV9-Naglu delivery

Aside from primary lysosomal dysfunction, our work underscores that another important contributor to MPSIIIB pathology is the activation of brain resident phagocytes, also known as microglial cells. Of the genes identified by microarray analysis as differentially expressed in untreated MPSIIIB mice, the vast majority of them were associated with inflammation and innate immunity. Furthermore, when the same microarray data were subjected to Cell Type Enrichment (CTEN) analysis—a software that assesses the contribution of each cell type to the changes in the transcriptome—the highest score was obtained for microglial cells, indicating that microglial activation was largely responsible for the observed changes in gene expression in untreated MPSIIIB brains. Neuroinflammation is a hallmark of human and animal MPSIIIB (5,6,28,33,74), in which an increase in the number and activation status of microglial cells has been described as early as 10 days postnatal (74). *In vitro* and *in vivo* studies have shown that partially catabolized HS can prime the activation of microglial cells through the components of the innate immune system Toll-like receptor 4 (TLR4) and TLR adaptor protein MyD88 (74). Although HS derivatives might be a primary and early inducer of microglial priming, the fact this activation is attenuated but not completely abolished in TLR4 or MyD88 deficient MPSIIIB mice (74) suggests that as disease progresses other signals released during cell damage/death could contribute to the establishment of chronic inflammatory disease in the MPSIIIB brain. Alternatively, activation of microglial cells may be triggered by factors endogenous to microglial cells. Our TEM analysis of the cortex of MPSIIIB mice suggests that this cell type is subjected to a heavier storage burden than neuronal cells, and the possibility that microglia act as a sink to buffer pathological accumulation in neurons has previously been proposed (71). Regardless of the activation trigger, microglia appear to play a proinflammatory role in MPS and participate in neurodegeneration through multiple mechanisms such as secretion of molecules that are toxic to neurons or production of reactive oxygen species (30,33,54,74). An important finding of our study is that upon treatment with AAV9-*Naglu* vectors, the expression of the majority of genes associated with microglia was normalized, an observation in agreement with the disappearance of BSI-B4-positive cells from different brain areas and the clearance of large storage vacuoles from the cytoplasm of perineuronal glial cells of the cortex of treated MPSIIIB animals. Our co-localization studies in mice and dogs (25) indicate that AAV9 vectors do not transduce microglial cells when delivered to the CSF. Therefore, the only possible mechanism to explain the extensive correction of lysosomal pathology documented in this cell population is cross-correction, by which non-transduced microglial cells recapture the NAGLU produced by other cells and target it to their lysosomes. The observed treatment-mediated complete resolution of inflammation is at the same time indicating that the causes and consequences of microglial activation are no longer present in the brain of treated animals.

Reversibility of MPSIIIB disease

The high levels of enzymatic activity achieved with intra-CSF AAV9-*Naglu* therapy mediated full correction of MPSIIIB disease. A significant extension of the expected lifespan was also observed; while untreated or Null-injected animals were all dead by 15–16 months of age, some treated MPSIIIB males and females lived >2 years. However, life expectancy was slightly shorter than for healthy littermates. This observation could be attributed to the fact that we used 2-month-old MPSIIIB animals in our studies, an age considered roughly equivalent to a 12–16-year-old-child (75). At this stage of the disease, the cascade of pathological events that are triggered by lysosomal dysfunction have long been initiated (74). Some of these changes might be completely reversible, as demonstrated here by the observation of full biochemical, histological and functional correction of the disease phenotype, most strikingly with normalization of behavioural deficits that were already present at treatment. Although the progression of MPSIIIB disease may be different in rodents and humans, and the animal model used here has no residual NAGLU

activity and could therefore be regarded as an extreme pheno-type, our study also suggests that the reversal of certain patho-physiological processes may require earlier intervention. This concept might be of particular relevance in the context of neuro-degenerative diseases and is supported by results from a clinical gene therapy study for Leber Congenital Amaurosis that showed that efficacy decreased with the age at treatment (76).

Impact of pre-existing anti-AAV immunity on intra-CSF AAV9-mediated transduction

The CSF bathes the whole CNS and can distribute substances delivered intrathecally to areas of difficult access. The periodic administration of recombinant α-Iduronidase (Aldurazyme®) and Iduronate-2-sulphatase (Elaprase®) to the CSF circumvents the BBB and is indicated in cases of cognitive decline or spinal cord compression in MPSI and II patients (77,78). At the moment, the strategy is under preclinical testing for MPSIIIB and is being assayed in the clinic for neurological MPSIIIA (NTC01155778 and NTC01299727, clinicaltrials.gov). Gene therapy provides a way of achieving sustained *in situ* production of the therapeutic protein after a single administration eliminating the need for periodic lumbar administrations under anaesthesia or the risks associated with the implantation of intrathecal delivery devices (IDD). However, one of the most important limitations to the de-velopment of *in vivo* gene therapies with AAV vectors is the pres-ence of anti-AAV humoral immunity in the majority of the population (56). In the case of AAV9 vectors, the incidence and ti-tres of anti-AAV9 antibodies are lower than for other commonly used serotypes (56). In addition, the target population in MPSIIIB is paediatric and children tend to have lower antibody titres than adults (79,80). Yet, the evidence showing that very low titres of NAbs is sufficient to completely block transduction upon sys-temic administration (57–59) highlights the need for the careful evaluation of CNS transduction in animals with pre-existing im-munity. Anti-AAV NAbs seem to have only a marginal effect on CNS transduction via the CSF, although studies previously per-formed in large seropositive animals utilized GFP, a non-secreted transgene (25,81) making it difficult to evaluate the impact of anti-AAV antibodies on the CSF levels of therapeutic proteins. Therefore, an important finding of our study is that a single intra-CSF administration of NAGLU-encoding vectors led to detection of active enzyme in the CSF of dogs with pre-existing immunity at levels that were indistinguishable from those achieved in naïve dogs, and this is a clear advantage over approaches based on systemic delivery of vectors. Furthermore, the fact that dogs with high-titre serum NAbs (>1:1000) had un-detectable levels of NAbs in the CSF opens the possibility for re-administration of vector to this compartment. Even though CNS efficacy is not lost following vector delivery to the CSF in animals with circulating anti-AAV NAbs, transduction of somatic organs is completely abolished (25). A combined therapy based on gene delivery to treat CNS disease and ERT to treat systemic path-ology can be envisioned as a therapeutic alternative for patients seropositive for anti-AAV9 antibodies.

Concluding remarks

In summary, the present work provides strong evidence support-ing the use of AAV9 vectors encoding for NAGLU delivered to the CSF as a therapeutic strategy for MPSIIIB. The administration of the therapeutic vector to MPSIIIB mice at an age at which animals already show behavioural impairment resulted in restoration of enzymatic activity, normalization of GAG content and lysosomal

physiology and eradication of neuroinflammation from the CNS of treated mice of both genders. In addition, the passage of vec-tors to the circulation and the subsequent transduction of the liver resulted in correction of peripheral disease. Treated animals behaved normally and lived significantly longer than untreated littermates demonstrating the efficacy of the therapy. Moreover, studies conducted in large animals indicate that this efficacy, at least at CNS level, would not be lost if the therapeutic vector is ad-ministered to individuals with pre-existing immunity against AAV9.

Materials and Methods

Animals

Congenic C57Bl/6 mice carrying a targeted mutation in the *Naglu* gene were used. Affected MPSIIIB and healthy littermates were bred from heterozygous founders (The Jackson Laboratory, MA, USA). Genotyping was performed by PCR following provider's in-structions. Mice were fed *ad libitum* with standard diet (Harlan–Teklad) and maintained under light–dark cycle of 12 h. Male healthy Beagle dogs (Isoquimen, Spain) were fed individually once daily at 9:00 AM with 30 g/kg body weight standard dry food (Elite Nutrition, Nestle).

AAV vector production and administration

AAV expression cassettes were generated by cloning the opti-mized coding sequence of murine or canine N-acetylglucosami-nidase, alpha (GeneArt; Life Technologies) under the control of the ubiquitous CAG promoter (hybrid of chicken β-actin promoter and CMV enhancer) into single-stranded AAV backbone plas-mids. Vectors were produced by optimized triple transfection protocol (82). Delivery of vectors to mice and dogs was performed as previously described (25). Mice were dosed with the same number of vector genomes/mouse irrespective of gender or body weight. The dose used in dogs was escalated from mice based on brain volume (83,84). All experimental procedures were approved by the Ethics Committee for Animal and Human Experimentation of Universitat Autònoma de Barcelona.

Activity of lysosomal enzymes

Mice were anaesthetized with Ketamine and Xylazine (100 and 10 mg/kg, respectively), blood was extracted by cardiac puncture, and animals were intracardiacally perfused with 12 ml of PBS to clear blood from tissues. Brain and liver samples were sonicated in 500 μl water and enzyme activities were determined in super-natants using 4-methylumbelliferone-derived fluorogenic sub-strates. NAGLU activity was assayed as previously described (85). Briefly, 30 μg of tissue protein extract, or 10 μl of serum or canine CSF, were incubated with 2.5 nmol/l 4-methylumbelliferyl-α-D-N-acetyl-glucosaminide (MU-αGlcNAc, Moscerdam Sub-strates) for 3 h at 37°C. IDUA activity was measured in 15 μg of protein incubated for 1 h at 37°C with 4-methylumbelliferyl α-L-iduronide (Glycosynth). For IDS activity, 15 μg of protein were first incubated with 4-methylumbelliferyl-α-L-iduronide-2-sulphate (Moscerdam Substrates) for 4 h at 37°C, followed by a second 24 h incubation at 37°C with a pool of lysosomal enzymes from bovine testis (LEBT-M2, Moscerdam Substrates). SGSH activity was mea-sured as previously described (25). For GUSB activity, 10 μg of pro-tein were incubated with 4-methylumbelliferyl-β-D-glucuronide (Sigma) at 37°C for 1 h. HEXB activity was assayed by incubation of 0.1 μg of protein with 4-methylumbelliferyl N-acetyl-β-D-gluco-saminide (Sigma) for 1 h at 37°C. After stopping reactions by

increasing the pH, released fluorescence was measured with FLx800 fluorimeter (BioTek Instruments). All enzyme activities were normalized against volume of CSF or serum, or against total protein content quantified by Bradford (Bio-Rad).

GAG quantification

Tissues were digested overnight with proteinase K (0.2 mg/ml) and extracts were clarified by centrifugation and filtration with 0.22 μm microporus membrane-containing filters (Ultrafree MC, Millipore). GAGs were measured with a commercially available kit (Biocolor). Chondroitin 4-sulphate was used as standard and values were normalized to wet tissue weight.

Histology and electron microscopy

Tissues were fixed in formalin, embedded in paraffin, sectioned in 4–6 μm slices and incubated overnight at 4°C with the following primary antibodies: rat anti-LAMP1 (SC-1992, Santa Cruz Biotechnology), rabbit anti-LIMP2 (NB400, Novus Biologicals), rabbit anti-GFAP (Z0334, Dako Cytomation), mouse anti-NeuN (MAB377, Millipore), goat anti-Iba1 (ab5076, Abcam), goat anti-GFP (ab6673, Abcam), chicken anti-GFP (ab13970, Abcam) and goat anti-TFEB (ab2636, Abcam) antibodies. Staining with peroxidase-conjugated BSI-B4 lectin was used to detect microglia (L5391, Sigma). Biotinylated rabbit anti-rat IgG (E0467, Dako), Donkey Anti-Chicken IgY H&L (FITC) (ab63507, Abcam) or biotinylated goat anti-rabbit IgG (31820, Vector Laboratories) were used as secondary antibodies. Sections were stained with 3,3-diaminobenzidine (Sigma) and counterstained with haematoxylin. When required, nuclei were counterstained with Hoechst (B2261, Sigma). Images were obtained with an Eclipse 90i optical microscope (Nikon) or a confocal microscope (Leyca Microsystems). LIMP2, GFAP and BSI-B4 signals were quantified with the NIS-Elements Advanced Research 2.20 software in 3–5 ×20 images/animal of each brain region using the same signal threshold settings for all animals. The percentage area of each image that had positive signal was then calculated. Samples for transmission electron microscopy were processed as previously described (50) and analysed with a Hitachi H-7000 transmission electron microscope (Hitachi).

Vector biodistribution

Tissues were digested overnight in Proteinase K (0.2 mg/ml) and total DNA was isolated with MasterPureDNA Purification Kit (Epicentre Biotechnologies). Vector genome copy numbers were determined in triplicates in 20 ng of DNA by qPCR with primers and probe specific for optimized murine *Naglu* coding sequence, which do not recognize endogenous *Naglu*. Forward primer: 5′-GCC GAG GCC CAG TTC TAC-3′; reverse primer: 5′-TTG GCG TAG TCC AGG ATG TTG-3′; probe: 5′-AGC AGA ACA GCA GAT ACC AGA TCA CCC-3′. Vgs/sample were interpolated from a standard curve built by serial dilutions of a linearized plasmid bearing optimized murine NAGLU expression cassette spiked into 20 ng of non-transduced genomic DNA.

Transcriptomic analysis

Half mouse brain (∼250 mg) was mechanically homogenized and total RNA was isolated with mirVana™ (Ambion, Life Technologies). cDNA was synthesized and subsequently hybridized in the GeneChip Mouse Gene 2.1 ST 16 array plate (Affymetrix) by Progenika Biopharma (Spain); sample processing, hybridization and scanning were carried out following Affymetrix recommended protocols and equipment. Data normalization was done by RMA (Robust Multiarray averaging) method using Affymetrix® Expression Console TM tool, obtaining $\log_2$ transformed normalized values. Data were filtered to focus the analysis on known coding sequences, obtaining an initial list of 26 688 altered genes, which were subsequently re-filtered to remove genes with variance below the 75th percentile. This process generated a working list of 6672 genes. For differentially expressed genes, FDR (False Discovery Rate) criteria <0.1 with 80% confidence was established. For clustering analysis, data were standardized and represented as heatmap using the J-Express Pro software (jexpress.bioinfo.no). Functional analysis was performed using Genecodis Tool 2.0 (genecodis2.dacya.ucm.es). Array data have been submitted to ArrayExpress database (http://www.ebi.ac.uk/arrayexpress/; accession code: E-MTAB-2984).

Neutralizing antibodies

NAb titres were determined in paired CSF and serum samples from dogs using an *in vitro* neutralization assay previously described (57). Briefly, 2V6.11 cells (ATCC), which express the adenoviral gene E4 under the control of an inducible promoter, were seeded in a 96-well plate at a density of 1.25×10^4 cells/well and ponasterone A at 1 mg/ml (Invitrogen) was added to the medium to induce E4 expression. Serial dilutions of heat-inactivated test serum were mixed with medium containing a self-complementary AAV9 vector carrying the Renilla luciferase reporter gene under the control of the chicken β-actin promoter. Residual activity of the reporter transgene was measured using a luminometer.

Open-field test

Animals were placed in the lower left corner of a brightly lit chamber (41 × 41 × 30 cm). The surface of the arena was divided in three concentric squares: centre (14 × 14 cm), periphery (27 × 27 cm) and border (41 × 41 cm). Exploratory behaviour and general activity were recorded during the first two minutes using a video-tracking system (Smart Junior, Panlab). The test was always performed at the same time of day (9:00 am to 1:00 pm) to minimize influence of circadian cycles.

Statistical analysis

All results are expressed as mean ± SEM. Statistical comparisons were made using one-way analysis of variance (ANOVA) and multiple comparisons between control and treatment groups were made using the Dunnett post-test. Statistical significance was considered if $P < 0.05$. Kaplan–Meier curves were used to estimate survival and the log-rank test was used for comparisons.

Supplementary Material

Supplementary Material is available at *HMG* online.

Acknowledgements

References

1. Von Figura, K. (1977) Human alpha-n-acetylglucosaminidase. 2. Activity towards natural substrates and multiple recognition forms. *Eur. J. Biochem.*, **80**, 535–542.

2. Champion, K.J., Basehore, M.J., Wood, T., Destrée, A., Vannuffel, P. and Maystadt, I. (2010) Identification and characterization of a novel homozygous deletion in the alpha-N-acetylglucosaminidase gene in a patient with Sanfilippo type B syndrome (mucopolysaccharidosis IIIB). *Mol. Genet. Metab.*, **100**, 51–56.

3. Yogalingam, G. and Hopwood, J.J. (2001) Molecular genetics of mucopolysaccharidosis type IIIA and IIIB: Diagnostic, clinical, and biological implications. *Hum. Mutat.*, **18**, 264–281.

4. Platt, F.M., Boland, B. and van der Spoel, A.C. (2012) The cell biology of disease: lysosomal storage disorders: the cellular impact of lysosomal dysfunction. *J. Cell Biol.*, **199**, 723–734.

5. Tamagawa, K., Morimatsu, Y., Fujisawa, K., Hara, A. and Taketomi, T. (1985) Neuropathological study and chemico-pathological correlation in sibling cases of Sanfilippo syndrome type B. *Brain Dev.*, **7**, 599–609.

6. Hamano, K., Hayashi, M., Shioda, K., Fukatsu, R. and Mizutani, S. (2008) Mechanisms of neurodegeneration in mucopolysaccharidoses II and IIIB: analysis of human brain tissue. *Acta Neuropathol.*, **115**, 547–559.

7. Valstar, M.J., Ruijter, G.J.G., van Diggelen, O.P., Poorthuis, B.J. and Wijburg, F.A. (2008) Sanfilippo syndrome: a mini-review. *J. Inherit. Metab. Dis.*, **31**, 240–252.

8. Neufeld, E.F. and Muenzer, J. (2001) The mucopolysaccharidoses. In Valle, D., Beaudet, A.L., Vogelstein, B., Kinzler, K.W., Antonarakis, S.E. and Ballabio, A. (eds), *The Online Metabolic and Molecular Bases of Inherited Disease*. McGraw-Hill, pp. 3421–3452.

9. Valstar, M.J., Bruggenwirth, H.T., Olmer, R., Wevers, R.A., Verheijen, F.W., Poorthuis, B.J., Halley, D.J. and Wijburg, F.A. (2010) Mucopolysaccharidosis type IIIB may predominantly present with an attenuated clinical phenotype. *J. Inherit. Metab. Dis.*, **33**, 759–767.

10. Van de Kamp, J.J., Niermeijer, M.F., von Figura, K. and Giesberts, M.A. (1981) Genetic heterogeneity and clinical variability in the Sanfilippo syndrome (types A, B, and C). *Clin. Genet.*, **20**, 152–160.

11. Meyer, A., Kossow, K., Gal, A., Mühlhausen, C., Ullrich, K., Braulke, T. and Muschol, N. (2007) Scoring evaluation of the natural course of mucopolysaccharidosis type IIIA (Sanfilippo syndrome type A). *Pediatrics*, **120**, e1255–e1261.

12. Moog, U., van Mierlo, I, van Schrojenstein Lantman-de Valk, H.M.J., Spaapen, L., Maaskant, M.A. and Curfs, L.M.G. (2007) Is Sanfilippo Type B in your mind when you see adults with mental retardation and behavioral problems? *Am J Med Genet Part C Semin Med Genet* **145C**, 293–301.

13. Zhao, H.G., Li, H.H., Bach, G., Schmidtchen, A. and Neufeld, E.F. (1996) The molecular basis of Sanfilippo syndrome type B. *Proc. Natl Acad. Sci. USA*, **93**, 6101–6105.

14. Enns, G.M. and Huhn, S.L. (2008) Central nervous system therapy for lysosomal storage disorders. *Neurosurg. Focus*, **24**, E12.

15. Kan, S.-h., Aoyagi-Scharber, M., Le, S.Q., Vincelette, J., Ohmi, K., Bullens, S., Wendt, D.J., Christianson, T.M., Tiger, P.M.N., Brown, J.R. *et al.* (2014) Delivery of an enzyme-IGFII fusion protein to the mouse brain is therapeutic for mucopolysaccharidosis type IIIB. *Proc. Natl Acad. Sci. USA*, **111**, 14870–14875.

16. Kan, S., Troitskaya, L.A., Sinow, C.S., Haitz, K., Todd, A.K., Di Stefano, A., Le, S.Q., Dickson, P.I. and Tippin, B.L. (2014) Insulin-like growth factor II peptide fusion enables uptake and lysosomal delivery of α-N-acetylglucosaminidase to mucopolysaccharidosis type IIIB fibroblasts. *Biochem. J.*, **458**, 281–289.

17. Ellinwood, N.M., Ausseil, J., Desmaris, N., Bigou, S., Liu, S., Jens, J.K., Snella, E.M., Mohammed, E.E.A., Thomson, C.B., Raoul, S. *et al.* (2011) Safe, efficient, and reproducible gene therapy of the brain in the dog models of Sanfilippo and Hurler syndromes. *Mol. Ther.*, **19**, 251–259.

18. Fu, H., Dirosario, J., Killedar, S., Zaraspe, K. and McCarty, D.M. (2011) Correction of neurological disease of mucopolysaccharidosis IIIB in adult mice by rAAV9 trans-blood-brain barrier gene delivery. *Mol. Ther.*, **19**, 1025–1033.

19. Murrey, D.A., Naughton, B.J., Duncan, F.J., Meadows, A.S., Ware, T.A., Campbell, K., Bremer, W.G., Walker, C., Goodchild, L., Bolon, B. *et al.* (2014) Feasibility and Safety of Systemic rAAV9-hNAGLU Delivery for Treating MPS IIIB: toxicology, bio-distribution and immunological assessments in primates. *Hum. Gene Ther. Clin. Dev.*, **25**, 72–84.

20. Souweidane, M.M., Fraser, J.F., Arkin, L.M., Sondhi, D., Hackett, N.R., Kaminsky, S.M., Heier, L., Kosofsky, B.E., Worgall, S., Crystal, R.G. *et al.* (2010) Gene therapy for late infantile neuronal ceroid lipofuscinosis: neurosurgical considerations. *J. Neurosurg. Pediatr.*, **6**, 115–122.

21. Tardieu, M., Zérah, M., Husson, B., de Bournonville, S., Deiva, K., Adamsbaum, C., Vincent, F., Hocquemiller, M., Broissand, C., Furlan, V. *et al.* (2014) Intracerebral administration of adeno-associated viral vector serotype rh.10 carrying human SGSH and SUMF1 cDNAs in children with mucopolysaccharidosis type IIIA disease: results of a phase I/II trial. *Hum. Gene Ther.*, **25**, 506–516.

22. Cressant, A., Desmaris, N., Verot, L., Bréjot, T., Froissart, R., Vanier, M.-T., Maire, I. and Heard, J.M. (2004) Improved behavior and neuropathology in the mouse model of Sanfilippo type IIIB disease after adeno-associated virus-mediated gene transfer in the striatum. *J. Neurosci.*, **24**, 10229–10239.

23. Inagaki, K., Fuess, S., Storm, T.A., Gibson, G.A., Mctiernan, C.F., Kay, M.A. and Nakai, H. (2006) Robust systemic transduction with AAV9 vectors in mice: efficient global cardiac gene transfer superior to that of AAV8. *Mol. Ther.*, **14**, 45–53.

24. Duque, S., Joussemet, B., Riviere, C., Marais, T., Dubreil, L., Douar, A.-M., Fyfe, J., Moullier, P., Colle, M.-A. and Barkats, M. (2009) Intravenous administration of self-complementary AAV9 enables transgene delivery to adult motor neurons. *Mol. Ther.*, **17**, 1187–1196.

25. Haurigot, V., Marcó, S., Ribera, A., Garcia, M., Ruzo, A., Villacampa, P., Ayuso, E., Añor, S., Andaluz, A., Pineda, M. *et al.* (2013) Whole body correction of mucopolysaccharidosis IIIA by intracerebrospinal fluid gene therapy. *J. Clin. Invest.*, **123**, 3254–3271.

26. Hinderer, C., Bell, P., Gurda, B.L., Wang, Q., Louboutin, J.-P., Zhu, Y., Bagel, J., O'Donnell, P., Sikora, T., Ruane, T. *et al.* (2014) Intrathecal gene therapy corrects CNS pathology in a feline model of mucopolysaccharidosis I. *Mol. Ther.*, **22**, 2018–2027.

27. Li, H.H., Yu, W.H., Rozengurt, N., Zhao, H.Z., Lyons, K.M., Anagnostaras, S., Fanselow, M.S., Suzuki, K., Vanier, M.T. and Neufeld, E.F. (1999) Mouse model of Sanfilippo syndrome type B produced by targeted disruption of the gene encoding alpha-N-acetylglucosaminidase. *Proc. Natl Acad. Sci. USA*, **96**, 14505–14510.

28. Ohmi, K., Greenberg, D.S., Rajavel, K.S., Ryazantsev, S., Li, H.H. and Neufeld, E.F. (2003) Activated microglia in cortex of mouse models of mucopolysaccharidoses I and IIIB. *Proc. Natl Acad. Sci. USA*, **100**, 1902–1907.

29. Canal, M.M., Wilkinson, F.L., Cooper, J.D., Wraith, J.E., Wynn, R. and Bigger, B.W. (2010) Circadian rhythm and suprachiasmatic nucleus alterations in the mouse model of mucopolysaccharidosis IIIB. *Behav. Brain Res.*, **209**, 212–220.

30. Villani, G.R.D., Gargiulo, N., Faraonio, R., Castaldo, S., Gonzalez, E. and Di Natale, P. (2007) Oxidative stress in brain disease from mucopolysaccharidosis IIIB. *J. Neurosci. Res.*, **85**, 612–622.

31. Heldermon, C.D., Hennig, A.K., Ohlemiller, K.K., Ogilvie, J.M., Herzog, E.D., Breidenbach, A., Vogler, C. and Wozniak, D.F. (2007) Development of sensory, motor and behavioral deficits in the murine model of Sanfilippo syndrome type B. *PLoS One*, **2**, e772.

32. McCarty, D.M., DiRosario, J., Gulaid, K., Killedar, S., Oosterhof, A., van Kuppevelt, T.H., Martin, P.T. and Fu, H. (2011) Differential distribution of heparan sulfate glycoforms and elevated expression of heparan sulfate biosynthetic enzyme genes in the brain of mucopolysaccharidosis IIIB mice. *Metab. Brain Dis.*, **26**, 9–19.

33. Wilkinson, F.L., Holley, R.J., Langford-Smith, K.J., Badrinath, S., Liao, A., Langford-Smith, A., Cooper, J.D., Jones, S.A., Wraith, J.E., Wynn, R.F. *et al.* (2012) Neuropathology in mouse models of mucopolysaccharidosis type I, IIIA and IIIB. *PLoS One*, **7**, e35787.

34. Fu, H., Bartz, J.D., Stephens, R.L. and McCarty, D.M. (2012) Peripheral nervous system neuropathology and progressive sensory impairments in a mouse model of Mucopolysaccharidosis IIIB. *PLoS One*, **7**, e45992.

35. Naughton, B.J., Duncan, F.J., Murrey, D., Ware, T., Meadows, A., McCarty, D.M. and Fu, H. (2013) Amyloidosis, synucleinopathy, and prion encephalopathy in a neuropathic lysosomal storage disease: the CNS-biomarker potential of peripheral blood. *PLoS One*, **8**, e80142.

36. Yu, W.H., Zhao, K.W., Ryazantsev, S., Rozengurt, N. and Neufeld, E.F. (2000) Short-term enzyme replacement in the murine model of Sanfilippo syndrome type B. *Mol. Genet. Metab.*, **71**, 573–580.

37. Zheng, Y., Ryazantsev, S., Ohmi, K., Zhao, H.-Z., Rozengurt, N., Kohn, D.B. and Neufeld, E.F. (2004) Retrovirally transduced bone marrow has a therapeutic effect on brain in the mouse model of mucopolysaccharidosis IIIB. *Mol. Genet. Metab.*, **82**, 286–295.

38. Di Natale, P., Di Domenico, C., Gargiulo, N., Castaldo, S., Gonzalez Y Reyero, E., Mithbaokar, P., De Felice, M., Follenzi, A., Naldini, L. and Villani, G.R.D. (2005) Treatment of the mouse model of mucopolysaccharidosis type IIIB with lentiviral-NAGLU vector. *Biochem. J.*, **388**, 639–646.

39. McCarty, D.M., DiRosario, J., Gulaid, K., Muenzer, J. and Fu, H. (2009) Mannitol-facilitated CNS entry of rAAV2 vector significantly delayed the neurological disease progression in MPS IIIB mice. *Gene Ther.*, **16**, 1340–1352.

40. Heldermon, C.D., Ohlemiller, K.K., Herzog, E.D., Vogler, C., Qin, E., Wozniak, D.F., Tan, Y., Orrock, J.L. and Sands, M.S. (2010) Therapeutic efficacy of bone marrow transplant, intracranial AAV-mediated gene therapy, or both in the mouse model of MPS IIIB. *Mol. Ther.*, **18**, 873–880.

41. Fu, H., DiRosario, J., Kang, L., Muenzer, J. and McCarty, D.M. (2010) Restoration of central nervous system alpha-N-acetyl-glucosaminidase activity and therapeutic benefits in mucopolysaccharidosis IIIB mice by a single intracisternal recombinant adeno-associated viral type 2 vector delivery. *J. Gene Med.*, **12**, 624–633.

42. Heldermon, C.D., Qin, E.Y., Ohlemiller, K.K., Herzog, E.D., Brown, J.R., Vogler, C., Hou, W., Orrock, J.L., Crawford, B.E. and Sands, M.S. (2013) Disease correction by combined neonatal intracranial AAV and systemic lentiviral gene therapy in Sanfilippo Syndrome type B mice. *Gene Ther.*, **20**, 913–921.

43. Bailey, K.R. and Crawley, J.N. (2009) Anxiety-related behaviors in mice. In *Methods of Behavior Analysis in Neuroscience*. 2nd edn. CRC Press, Boca Raton, FL.

44. Hemsley, K.M., Luck, A.J., Crawley, A.C., Hassiotis, S., Beard, H., King, B., Rozek, T., Rozaklis, T., Fuller, M. and Hopwood, J.J. (2009) Examination of intravenous and intra-CSF protein delivery for treatment of neurological disease. *Eur. J. Neurosci.*, **29**, 1197–1214.

45. Ruzo, A., Marcó, S., García, M., Villacampa, P., Ribera, A., Ayuso, E., Maggioni, L., Mingozzi, F., Haurigot, V. and Bosch, F. (2012) Correction of pathological accumulation of glycosaminoglycans in central nervous system and peripheral tissues of MPSIIIA mice through systemic AAV9 gene transfer. *Hum. Gene Ther.*, **23**, 1237–1246.

46. Sardiello, M., Palmieri, M., di Ronza, A., Medina, D.L., Valenza, M., Gennarino, V.A., Di Malta, C., Donaudy, F., Embrione, V., Polishchuk, R.S. *et al.* (2009) A gene network regulating lysosomal biogenesis and function. *Science*, **325**, 473–477.

47. Settembre, C., Fraldi, A., Medina, D.L. and Ballabio, A. (2013) Signals from the lysosome: a control centre for cellular clearance and energy metabolism. *Nat. Rev. Mol. Cell Biol.*, **14**, 283–296.

48. Eng, L.F. and Ghirnikar, R.S. (1994) GFAP and astrogliosis. *Brain Pathol.*, **4**, 229–237.

49. Streit, W.J. and Kreutzberg, G.W. (1987) Lectin binding by resting and reactive microglia. *J. Neurocytol.*, **16**, 249–260.

50. Ruzo, A., Garcia, M., Ribera, A., Villacampa, P., Haurigot, V., Marcó, S., Ayuso, E., Anguela, X.M., Roca, C., Agudo, J. *et al.* (2012) Liver production of sulfamidase reverses peripheral and ameliorates CNS pathology in mucopolysaccharidosis IIIA mice. *Mol. Ther.*, **20**, 254–266.

51. McGeer, P.L. and McGeer, E.G. (1998) Glial cell reactions in neurodegenerative diseases: pathophysiology and therapeutic interventions. Alzheimer Dis. Assoc. Disord., **12** (Suppl. 2), S1–E16.

52. Derecki, N.C., Cronk, J.C., Lu, Z., Xu, E., Abbott, S.B.G., Guyenet, P.G. and Kipnis, J. (2012) Wild-type microglia arrest pathology in a mouse model of Rett syndrome. *Nature*, **484**, 105–109.

53. DiRosario, J., Divers, E., Wang, C., Etter, J., Charrier, A., Jukkola, P., Auer, H., Best, V., Newsom, D.L., McCarty, D.M. *et al.* (2009) Innate and adaptive immune activation in the brain of MPS IIIB mouse model. *J. Neurosci. Res.*, **87**, 978–990.

54. Archer, L.D., Langford-Smith, K.J., Bigger, B.W. and Fildes, J.E. (2014) Mucopolysaccharide diseases: a complex interplay between neuroinflammation, microglial activation and adaptive immunity. *J. Inherit. Metab. Dis.*, **37**, 1–12.

55. Dickson, P., Peinovich, M., McEntee, M., Lester, T., Le, S., Krieger, A., Manuel, H., Jabagat, C., Passage, M. and Kakkis, E.D. (2008) Immune tolerance improves the efficacy of enzyme

replacement therapy in canine mucopolysaccharidosis I. *J. Clin. Invest.*, **118**, 2868–2876.

56. Boutin, S., Monteilhet, V., Veron, P., Leborgne, C., Benveniste, O., Montus, M.F. and Masurier, C. (2010) Prevalence of serum IgG and neutralizing factors against adeno-associated virus (AAV) types 1, 2, 5, 6, 8, and 9 in the healthy population: implications for gene therapy using AAV vectors. *Hum. Gene Ther.*, **21**, 704–712.

57. Manno, C.S., Pierce, G.F., Arruda, V.R., Glader, B., Ragni, M., Rasko, J.J., Rasko, J., Ozelo, M.C., Hoots, K., Blatt, P. et al. (2006) Successful transduction of liver in hemophilia by AAV-Factor IX and limitations imposed by the host immune response. *Nat. Med.*, **12**, 342–347.

58. Scallan, C.D., Jiang, H., Liu, T., Patarroyo-White, S., Sommer, J. M., Zhou, S., Couto, L.B. and Pierce, G.F. (2006) Human immunoglobulin inhibits liver transduction by AAV vectors at low AAV2 neutralizing titers in SCID mice. *Blood*, **107**, 1810–1807.

59. Jiang, H., Couto, L.B., Patarroyo-White, S., Liu, T., Nagy, D., Vargas, J.A., Zhou, S., Scallan, C.D., Sommer, J., Vijay, S. et al. (2006) Effects of transient immunosuppression on adeno-associated, virus-mediated, liver-directed gene transfer in rhesus macaques and implications for human gene therapy. *Blood*, **108**, 3321–3328.

60. Begley, D.J., Pontikis, C.C. and Scarpa, M. (2008) Lysosomal storage diseases and the blood-brain barrier. *Curr. Pharm. Des.*, **14**, 1566–1580.

61. Foust, K.D., Nurre, E., Montgomery, C.L., Hernandez, A., Chan, C.M. and Kaspar, B.K. (2009) Intravascular AAV9 preferentially targets neonatal neurons and adult astrocytes. *Nat Biotech*, **27**, 59–65.

62. Haurigot, V. and Bosch, F. (2013) Toward a gene therapy for neurological and somatic MPSIIIA. *Rare Dis. (Austin, Tex.)*, **1**, e27209.

63. Davidoff, A.M., Ng, C.Y.C., Zhou, J., Spence, Y. and Nathwani, A. C. (2003) Sex significantly influences transduction of murine liver by recombinant adeno-associated viral vectors through an androgen-dependent pathway. *Blood*, **102**, 480–488.

64. Binny, C., McIntosh, J., Della Peruta, M., Kymalainen, H., Tuddenham, E.G.D., Buckley, S.M.K., Waddington, S.N., McVey, J. H., Spence, Y., Morton, C.L. et al. (2012) AAV-mediated gene transfer in the perinatal period results in expression of FVII at levels that protect against fatal spontaneous hemorrhage. *Blood*, **119**, 957–966.

65. Desnick, R.J. (2004) Enzyme replacement and enhancement therapies for lysosomal diseases. *J. Inherit. Metab. Dis.*, **27**, 385–410.

66. Donsante, A., Levy, B., Vogler, C. and Sands, M.S. (2007) Clinical response to persistent, low-level beta-glucuronidase expression in the murine model of mucopolysaccharidosis type VII. *J. Inherit. Metab. Dis.*, **30**, 227–238.

67. Garcia, A.R., DaCosta, J.M., Pan, J., Muenzer, J. and Lamsa, J.C. (2007) Preclinical dose ranging studies for enzyme replacement therapy with idursulfase in a knock-out mouse model of MPS II. *Mol. Genet. Metab.*, **91**, 183–190.

68. Braunlin, E.A., Harmatz, P.R., Scarpa, M., Furlanetto, B., Kampmann, C., Loehr, J.P., Ponder, K.P., Roberts, W.C., Rosenfeld, H.M. and Giugliani, R. (2011) Cardiac disease in patients with mucopolysaccharidosis: presentation, diagnosis and management. *J. Inherit. Metab. Dis.*, **34**, 1183–1197.

69. McGlynn, R., Dobrenis, K. and Walkley, S.U. (2004) Differential subcellular localization of cholesterol, gangliosides, and glycosaminoglycans in murine models of mucopolysaccharide storage disorders. *J. Comp. Neurol.*, **480**, 415–426.

70. Walkley, S.U. (2004) Secondary accumulation of gangliosides in lysosomal storage disorders. *Semin. Cell Dev. Biol.*, **15**, 433–444.

71. Jolly, R.D., Johnstone, A.C., Norman, E.J., Hopwood, J.J. and Walkley, S.U. (2007) Pathology of mucopolysaccharidosis IIIA in Huntaway dogs. *Vet. Pathol.*, **44**, 569–578.

72. Wolfe, D.M., Lee, J.-H., Kumar, A., Lee, S., Orenstein, S.J. and Nixon, R.A. (2013) Autophagy failure in Alzheimer's disease and the role of defective lysosomal acidification. *Eur. J. Neurosci.*, **37**, 1949–1961.

73. Dehay, B., Martinez-Vicente, M., Caldwell, G.A., Caldwell, K. A., Yue, Z., Cookson, M.R., Klein, C., Vila, M. and Bezard, E. (2013) Lysosomal impairment in Parkinson's disease. *Mov. Disord.*, **28**, 725–732.

74. Ausseil, J., Desmaris, N., Bigou, S., Attali, R., Corbineau, S., Vitry, S., Parent, M., Cheillan, D., Fuller, M., Maire, I. et al. (2008) Early neurodegeneration progresses independently of microglial activation by heparan sulfate in the brain of mucopolysaccharidosis IIIB mice. *PLoS One*, **3**, e2296.

75. Barrow, P. (2007) Toxicology testing for products intended for pediatric populations. In Sietsema, W. and Schwen, R. (eds), *Non Clinical Drug Safety Assessment: Practical Considerations for Successful Registration*. Washington, DC, pp. 411–440.

76. Maguire, A.M., High, K.A., Auricchio, A., Wright, J.F., Pierce, E. A., Testa, F., Mingozzi, F., Bennicelli, J.L., Ying, G., Rossi, S. et al. (2009) Age-dependent effects of RPE65 gene therapy for Leber's congenital amaurosis: a phase 1 dose-escalation trial. *Lancet*, **374**, 1597–1605.

77. Jameson, E., Jones, S. and Wraith, J.E. (2013) Enzyme replacement therapy with laronidase (Aldurazyme) for treating mucopolysaccharidosis type I. *Cochrane Database Syst. Rev.*, **9**, CD009354.

78. Giugliani, R., Villarreal, M.L.S., Valdez, C.A.A., Hawilou, A.M., Guelbert, N., Garzón, L.N.C., Martins, A.M., Acosta, A., Cabello, J.F., Lemes, A. et al. (2014) Guidelines for diagnosis and treatment of Hunter Syndrome for clinicians in Latin America. *Genet. Mol. Biol.*, **37**, 315–329.

79. Calcedo, R., Morizono, H., Wang, L., McCarter, R., He, J., Jones, D., Batshaw, M.L. and Wilson, J.M. (2011) Adeno-associated virus antibody profiles in newborns, children, and adolescents. *Clin. Vaccine Immunol.*, **18**, 1586–1588.

80. Piguet, F., Sondhi, D., Piraud, M., Fouquet, F., Hackett, N.R., Ahouansou, O., Vanier, M.-T., Bieche, I., Aubourg, P., Crystal, R.G. et al. (2012) Correction of brain oligodendrocytes by AAVrh.10 intracerebral gene therapy in metachromatic leukodystrophy mice. *Hum. Gene Ther.*, **23**, 903–914.

81. Gray, S.J., Nagabhushan Kalburgi, S., McCown, T.J. and Jude Samulski, R. (2013) Global CNS gene delivery and evasion of anti-AAV-neutralizing antibodies by intrathecal AAV administration in non-human primates. *Gene Ther.*, **20**, 450–459.

82. Ayuso, E., Mingozzi, F. and Bosch, F. (2010) Production, purification and characterization of adeno-associated vectors. *Curr. Gene Ther.*, **10**, 423–436.

83. Davies, B. and Morris, T. (1993) Physiological parameters in laboratory animals and humans. *Pharm. Res.*, **10**, 1093–1095.

84. Ma, Y., Hof, P.R., Grant, S.C., Blackband, S.J., Bennett, R., Slatest, L., McGuigan, M.D. and Benveniste, H. (2005) A three-dimensional digital atlas database of the adult C57BL/6J mouse brain by magnetic resonance microscopy. *Neuroscience*, **135**, 1203–1215.

85. Marsh, J. and Fensom, A.H. (1985) 4-Methylumbelliferyl alpha-N-acetylglucosaminidase activity for diagnosis of Sanfilippo B disease. *Clin. Genet.*, **27**, 258–262.